GeoArabia, v. 14, no. 2, 2009, p. 17-44
Gulf PetroLink, Bahrain

Subsidence history, gravity anomalies and flexure of the United Arab Emirates (UAE) foreland basin

Mohammed Y. Ali and A. B. Watts

ABSTRACT

Seismic reflection profile, gravity anomaly, and exploratory well data have been used to determine the structure and evolution of the United Arab Emirates (UAE) foreland basin. The basin is of tectonic significance because it formed by ophiolite obduction in the northern Oman Mountains and flexural loading of an underlying Tethyan rifted margin. Existing stratigraphic data shows that this margin is characterised by an early syn-rift sequence of mainly Triassic age that is overlain by a post-rift sequence of Lower Jurassic to Upper Cretaceous age. Backstripping of the well data provides new constraints on the age of rifting, the amount of crustal and mantle extension, and the flexural effects of ophiolite load emplacement. The tectonic subsidence and uplift history at the wells can be generally explained by either a uniform extension model with an initial age of rifting of 210 Ma and a stretching factor, β, of 2.5 or a depth-dependant extension model with crustal extension factor of, γ, 1.3 and a mantle extension factor, β, of 2.5. While both models account for the general exponential decrease that is observed in the tectonic subsidence and uplift between 210 Ma and 95 Ma, we prefer the depth-dependant model because the depth-to-Moho that is implied better accounts for the increase that is observed in the regional Bouguer gravity anomaly between the UAE foreland and the Oman coastline. However, there are discrepancies, which we attribute to uncertainties in palaeobathymetry, sea level, and stratigraphic ages. Irrespective, the backstrip curves suggest that there was a significant thinning of the continental crust prior to ophiolite emplacement. The timing of emplacement cannot be constrained precisely, but the backstrip curves suggest that ophiolite loading and foreland basin flexure was initiated during the Late Cretaceous. The basin shape can be explained by a simple model in which both surface (i.e. topographic) and subsurface (i.e. ophiolitic) loads were emplaced on a lithosphere with an effective elastic thickness, T_e, of c. 20–25 km. This T_e is similar to what we would expect for loading of extended continental lithosphere 80 My after a rifting event. It predicts a c. 4 km flexural depression and a few hundred metres flanking bulge that is presently located beneath the Abu Dhabi region. The bulge is obscured, however, by at least 2 km of sediment, possibly because of an increase in accommodation space due to dynamic effects associated with the subduction of the Arabian Plate beneath the Eurasian Plate.

INTRODUCTION

Foreland basins form by lithospheric flexure in front of migrating thrust and fold loads (e.g. Price, 1971). They are usually "wedge-shaped" in cross-section and are infilled by sediments that have mainly been derived from the adjacent thrust and fold belt. The foreland basin is separated from the orogenic belt by a major thrust fault and from the cratonic interior by a peripheral bulge (e.g. DeCelles and Giles, 1996). There is evidence that the bulge may migrate across a foreland basin, both towards and away from the thrust and fold belt, and that they may, in some cases, act as a localised sediment source.

Gravity anomaly and flexure studies suggest that foreland basins form by surface (i.e. topographic) and subsurface (i.e. buried) loading (e.g. Karner and Watts, 1983). Surface loads comprise the ramps that form thrust and folds, and although their geometry can be reconstructed from balanced cross-sections, they are usually approximated by the present-day topography. The origin of buried loads is not as clear, but examples include intra-crustal thrusting (Lin and Watts, 2002), ophiolite obduction

(Corfield et al., 2005), and dense downgoing slabs (Royden and Karner, 1984). Burgess and Moresi (1999) and Liu and Nummedal (2004), among others, have suggested that dynamic topography due to slab subduction maybe an important additional contributor to foreland basin flexure.

Foreland basins comprise a distinct stratigraphic 'architecture', usually involving onlap as clastic clinoform wedges move out across the basin and then offlap as the depositional centre migrates in towards the surface and buried loads and the basin fills. Forward modelling studies have shown that the patterns of onlap and offlap are mainly controlled by the rate of migration of the thrust and fold belt, the flexural response of the underlying basement, and the rate of sediment flux into the basin (e.g. Jordan, 1981; Flemings and Jordan, 1989; Sinclair et al., 1991).

Previous studies (e.g. Robertson, 1987a; Patton and O'Connor, 1988; Boote et al., 1990; Warburton et al., 1990; Ali et al., 2008) suggest that the United Arab Emirates (UAE) foreland basin developed by flexural loading of an underlying rifted continental margin. The rifted margin sequence (that includes Araej, Sila, Thamama and Wasia groups) comprise predominantly shelf carbonates with minor deposits of evaporites and clastics that formed during the Permian to mid-Cretaceous following break-up of the Arabian Plate and Cimmerian Terrane as well as the formation of Neo-Tethyan oceanic crust (Glennie et al., 1973; Searle, 1988a; Ruban et al., 2007) (Figures 1 and 2). The foreland basin (or Aruma basin) sequence comprises mainly deep-marine mudstones of the Fiqa and Juwaiza formations that formed during the Late Cretaceous (Late Coniacian to Campanian) subsequent to ophiolite emplacement and thrust and fold loading in the Oman Mountains.

Although there have been a number of stratigraphic studies of the rifted margin sequences that are exposed in the eastern UAE and northern Oman Mountains (e.g. Robertson, 1987b; Searle, 1988b; Rabu et al., 1993; Styles, et al., 2006; Searle, 2007), there have been few quantitative studies of their subsidence and uplift history. As a result, we know little about the thermal and mechanical properties of the Neo-Tethyan rifted margin. One problem has been that the exposures are deformed and so it is difficult to restore their thickness. The best record of the subsidence and uplift history, we believe, is in the relatively undeformed rifted margin sequences that underlie the UAE foreland basin.

The main aims of this paper is to use seismic reflection profile, exploratory well, and Bouguer gravity anomaly data, together with modern basin analysis techniques, to determine the tectonic subsidence and uplift history of the rifted margin. We then examine its implications for the crustal structure, flexural strength and thermal history of the UAE foreland basin.

GEOLOGICAL SETTING

During the early Mesozoic, the UAE region was located in an equatorial setting as part of a large carbonate platform on the rifted southern continental margin of the Neo-Tethys Ocean. The early stages of rifting were in the Mid-Permian (Glennie et al. 1973; Béchennec et al., 1990), as is evidenced by the Jabal Qamar exotic in the Dibba Zone, and Mid-Permian syn-rift (Bih Formation) in the Musandum Peninsula, while the later stages were in the Late Triassic – Early Jurassic (Glennie et al., 1973; Searle et al., 1983; Searle, 1988b; Robertson et al., 1990; Béchennec et al., 1990). The early rift stage was dominated by continental rifting and block-faulting with more localised within-plate off-axis volcanism, while the later stage was characterised by volcanism, tilted fault blocks, half-grabens and growth on the main border faults, leading to break-up (Robertson and Searle, 1990). Further, geochemical analyses of volcanic rocks in Saih Hatat in the central Oman Mountains suggest that oceanic crust was formed in the Late Triassic (Searle, 2007).

By the end of the mid-Cretaceous, the region was a mature carbonate-dominated rifted margin in an expanding Neo-Tethys Ocean basin. However, at the end of the Late Cretaceous (from the Late Cenomanian to the end of the Early Maastrichtian), the region was subjected to compressional deformation. This involved the emplacement of a number of thrusts each of which was emplaced from NE to SW onto the Neo-Tethyan rifted continental margin (Glennie et al., 1973; Lippard et al., 1986; Searle, 1988a). The thrusts (e.g. Figures 1 and 2) comprise the Sumeini Complex, shelf-edge and slope-carbonate sediments; the Hawasina Complex, comprising distal-slope and deep-sea Neo-Tethyan sediments; Haybi Complex, comprising Permian to Cenomanian exotic limestones (Oman

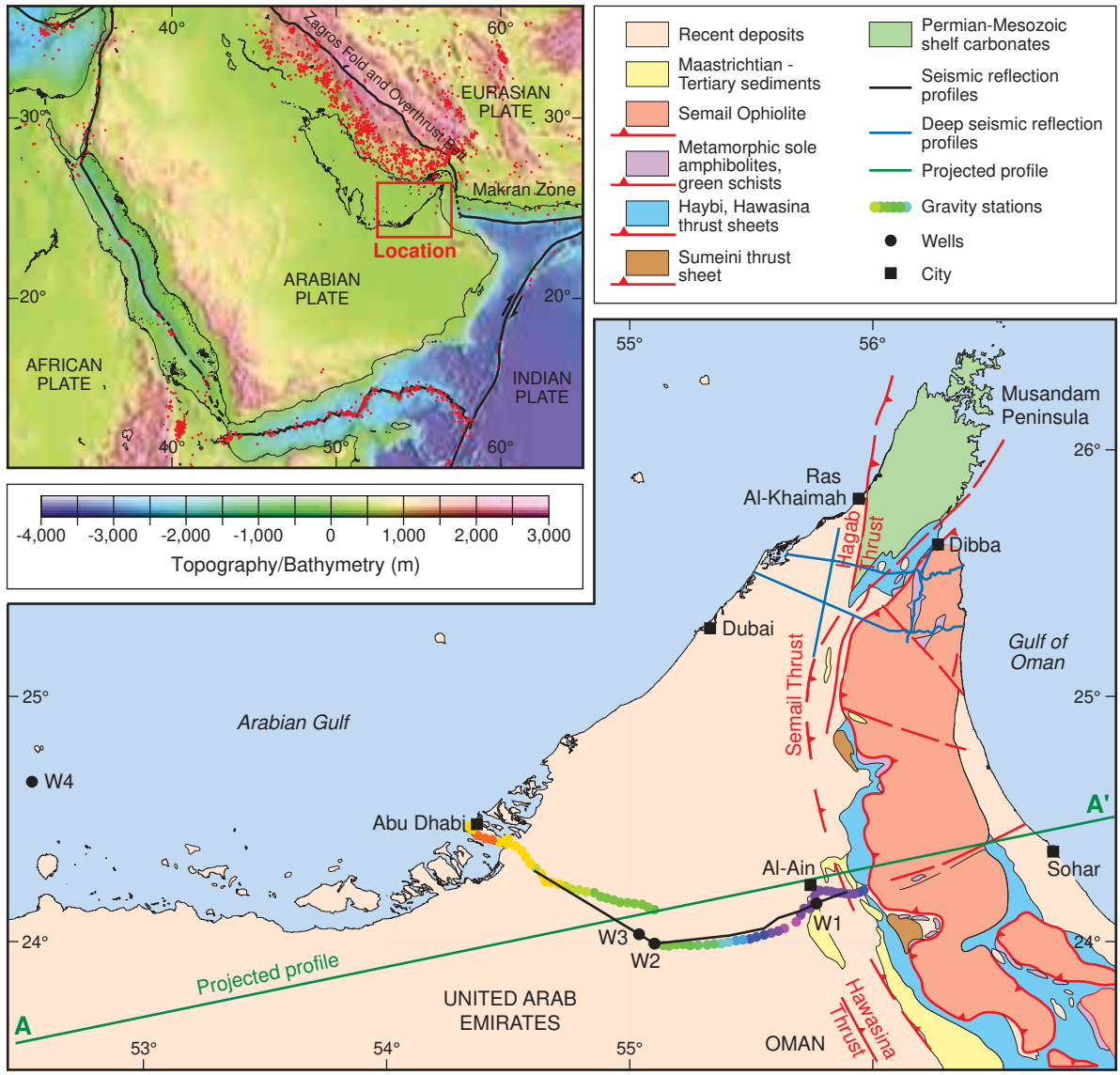

Figure 1: Summary geological map of the UAE foreland basin and northern Oman Mountains (Modified from Searle, 2007). The thick black lines, filled circles and colour-coded profile shows the location of the seismic reflection profiles, exploratory wells, and Bouguer gravity anomaly data used in this paper. The thick green line shows Profile AA', along which the data has been projected. The thick blue lines show the locations of deep seismic reflection profiles in the northern UAE (Roure et al., 2006).

exotics), volcanics (Haybi volcanics), mélanges, sub-ophiolitic metamorphic rocks, and the Semail Ophiolite complex, a massive 'slab' (up-to 8–15 km thick) of oceanic crust and mantle of Cenomanian – Turonian age, which formed above an east-dipping intra-oceanic subduction zone (Searle and Cox, 1999). The emplacement of thrust sheets was completed by 70 Ma (Early Maastrichtian) (Searle, 2007).

The obduction of the Semail Ophiolite and its associated thrusts and folds loaded and then flexed the pre-existing underlying rift margin sediments. The flexure formed the UAE foreland basin and flanking bulge, which together migrated westward in front of the advancing ophiolite load.

During obduction, the ophiolite was intensely deformed, but the underlying Mesozoic shelf carbonates remained relatively undeformed, except for minor extensional faulting (Warburton et al., 1990; Boote et al., 1990; Ali et al., 2008). However, in the peripheral bulge region, uplift and erosion of the shelf carbonates contributed to the Turonian Wasia-Aruma break that now separates the rifted margin

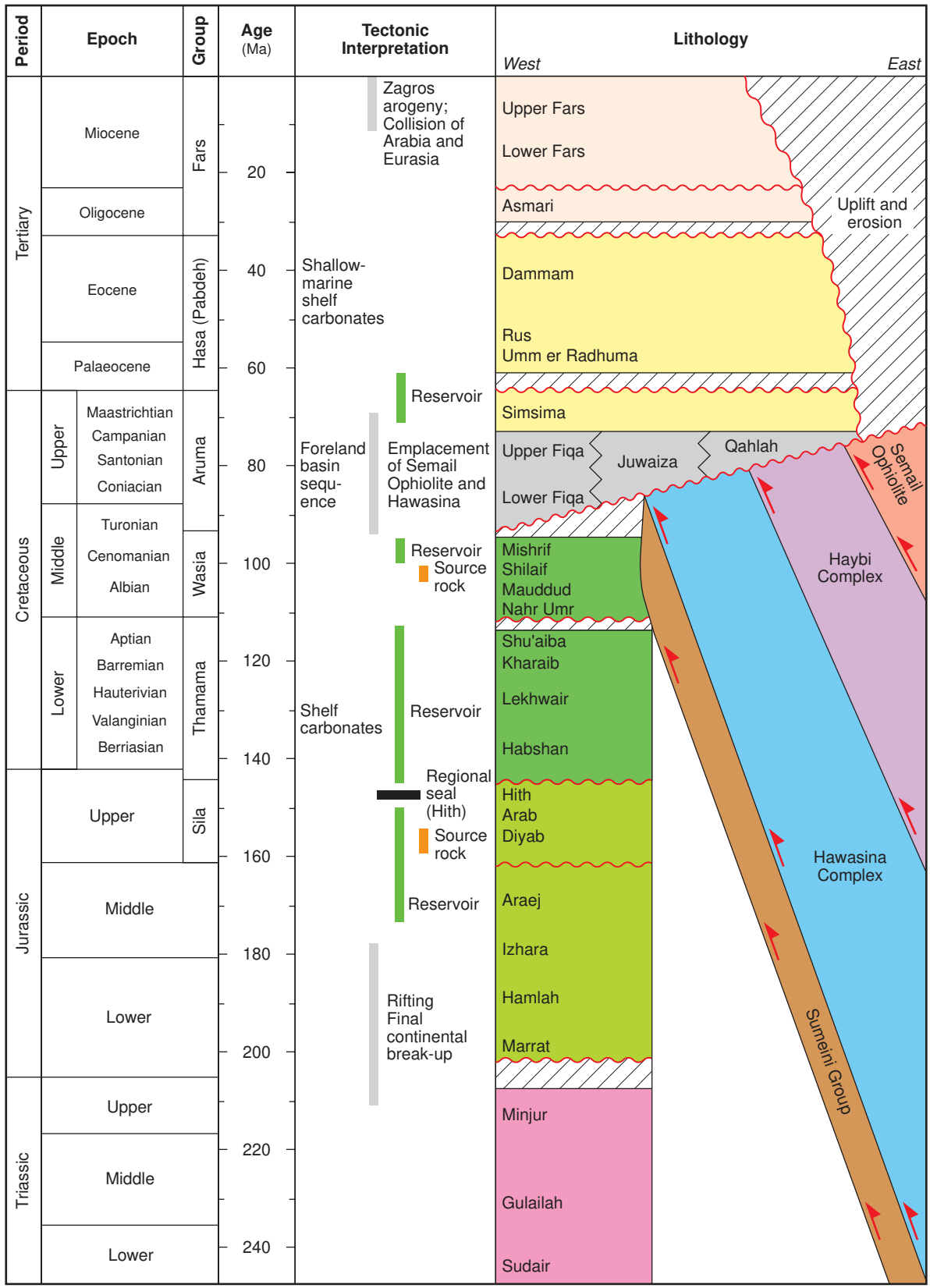

Figure 2: Summary of stratigraphic column of the UAE foreland basin. Modified from Ali et al. (2008).

sequence from the overlying foreland basin sequence. On the Lekhwair High and in the Sharjah (UAE) area a significant amount of uplift and erosion of shelf carbonates may have been caused by a peripheral bulge that developed in response to thrust and fold loading and flexure of the shelf carbonates (Robertson, 1987a; Patton and O'Connor, 1988).

The Upper Cretaceous foreland basin was infilled by an up to 4.3 km thick Santonian – Campanian deep-marine mudstones of the Fiqa and Juwaiza formations, which rapidly increase in thickness towards the northeast (Glennie et al., 1973). Seismic sections across the foreland show the Hawasina thrust tips extending up into the Fiqa Formation (Warburton et al., 1990; Boote et al., 1990; Ali et al., 2008). The foreland sequence is, in turn, overlain by the Upper Maastrichtian to Palaeogene conglomerates and shallow-marine limestone of the Qahlah and Simsima formations (Glennie et al., 1973; Lippard et al., 1986). The margin remained stable until post-Middle Eocene time through the deposition of the transgressive Umm Er Radhuma Formation.

The UAE foreland basin region was affected by a second compressional event during the Late Eocene – Miocene when the Arabian Plate moved northeastward, colliding with the Eurasian Plate (Searle et al., 1983, 1988b; Searle and Ali, 2009). This event produced large-scale fold 'culminations' and the re-activation of deep-seated faults in the frontal fold and thrust belt and adjacent foreland basin (Boote et al., 1990; Dunne et al., 1990; Searle et al., 1990; Searle and Ali, 2009). In addition, there was an uplift of at least 3 km along the western flank of the northern Oman Mountains (Boote et al., 1990). As a result, the sedimentary record was deeply eroded. However, the Tertiary deformation is recorded in the sequences that infill the foreland basin.

The regional geological structure of the UAE foreland basin and northern Oman Mountains are reflected in the Bouguer gravity anomaly map (Figure 3). The map, which was constructed from the contour data of Ravaut and Warsi (1997) in Oman and the newly acquired gravity data of Jordan (2007) and Savage (2007) in the UAE, reveals that the Oman Mountains south of the Dibba Fault Zone are associated with a N-S trending Bouguer gravity anomaly *high*. The high correlates with the ophiolite outcrop and reaches its maximum value along the UAE coastline, suggesting that the ophiolite may extend offshore. The *high* is flanked on its western edge by a N-S trending 'low' that reaches its minimum value over the UAE foreland basin. We attribute this gravity *high-low couple*, which dominates the Bouguer anomaly map, to ophiolite loading and flexure of the rifted Neo-Tethyan margin. The *couple* is flanked to the west - in the Arabian Gulf - by a small-amplitude long-wavelength *high*, which we believe delineates the present-day position of the outer bulge to this loading and flexure.

SEISMIC STRATIGRAPHY OF THE RIFTED MARGIN AND OVERLYING FORELAND BASIN

Figure 4a shows a W-E composite regional seismic reflection profile of the UAE foreland basin between Abu Dhabi in the west and Al-Ain in the east. The seismic data were acquired by WesternGeco and processed during the 1980s and 1990s as part of hydrocarbon exploration activities in the area. Also shown are the locations of three nearby exploration wells. The seismic data reveal the sedimentary structure of the basin, but does not distinguish the syn-rift sequence from the post-rift sequence or the underlying basement. Moreover, the wells only appear to penetrate the post-rift sequence. The combined seismic and well data, however, allow us to sub-divide the stratigraphy of the foreland basin into three major sequences. Each sequence was delineated (Figure 4b) on the basis of its seismic character, reflector terminations (e.g. onlap, toplap, and offlap) and structural style, inferred from continuity and amplitude of prominent reflectors (e.g. Mitchum et al., 1977; Sheriff and Geldart, 1995).

Mesozoic Shelf Carbonate Sequence (Wasia Group)

This sequence exhibits high-amplitude, continuous to discontinuous reflectors. In addition, the seismic profile suggests the presence of fault blocks that generally step up towards the mountain front. We do not recognise crystalline basement, but the regional Upper Turonian Wasia-Aruma break can be

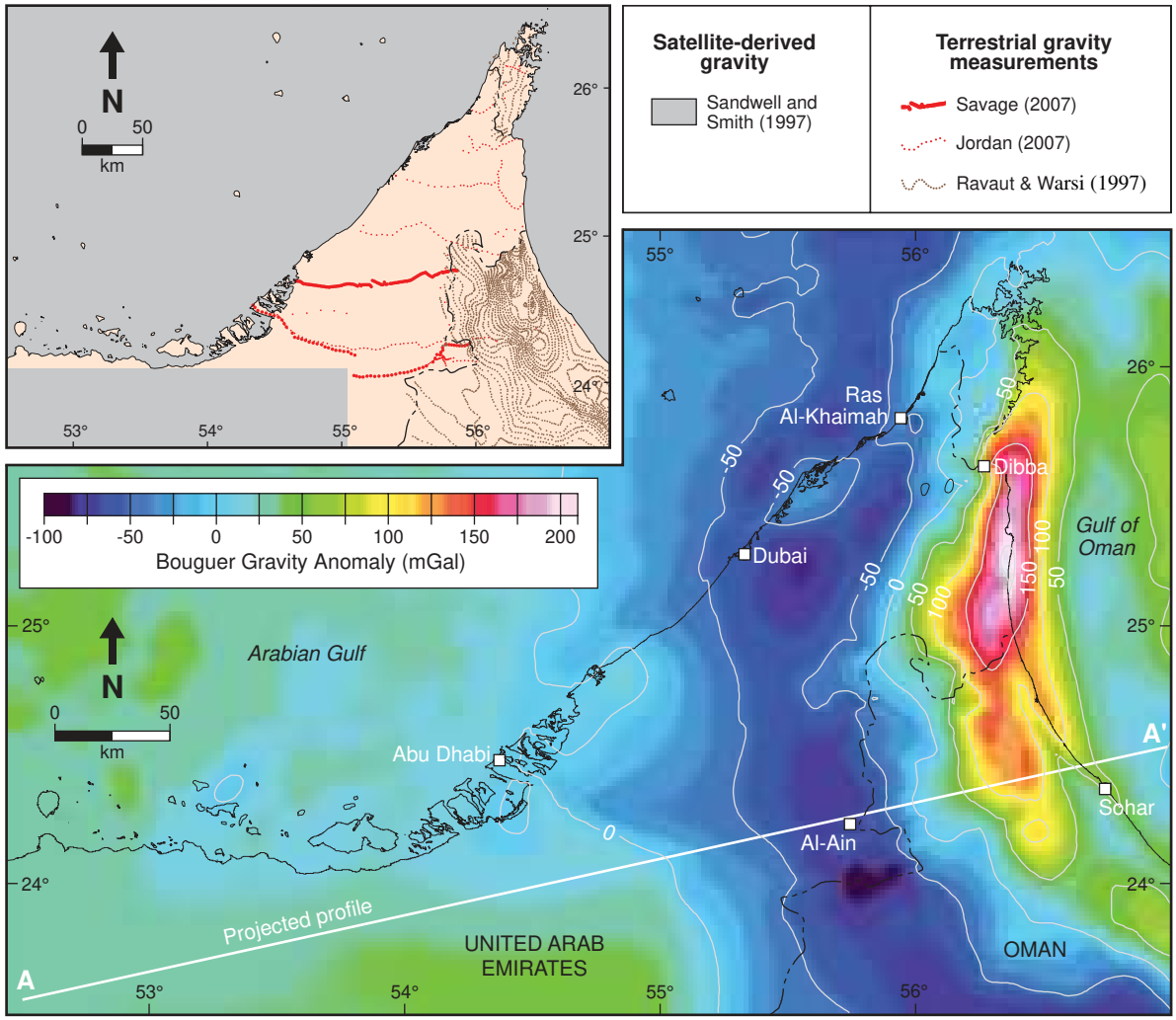

Figure 3: Bouguer gravity anomaly map of the UAE foreland basin and Oman Mountains. The Bouguer anomalies have been computed assuming a reduction density of 2,670 kg m^{-3}. The main sources of the data are shown in the inset. The thick white line shows projected Profile AA′.

tentatively identified as a local toplap and truncating terminations to Lower Fiqa reflectors. Boote et al. (1990) and Ali et al. (2008) interpreted these observations as the result of a period of plate margin rock uplift and erosion caused by the development of a flexural bulge during the initial phases of emplacement of the Semail Ophiolite and its associated thrusts and folds.

Foreland Basin Sequence (Upper Cretaceous)

This sequence is wedge shaped with a maximum thickness of c. 3 km (1.5 sec Two-Way Travel Time (TWTT)) close to the thrust front. There, the sequence displays internal seismic reflections showing a variable amplitude, discontinuous, low-frequency, low-vertical spacing as well as chaotic pattern. To the west, its reflection terminations indicate onlap geometries onto the underlying rifted margin while gradually pinching out further westwards. In its most western part, the sequence exhibits high-medium amplitude, continuous strong reflectors. We refer to this sequence as the Fiqa. The seismic data suggest that the lower part of the Fiqa was deposited immediately after the development of the foreland basin as a response to loading of the Semail Ophiolite and its associated thrust sheets. In contrast, the upper part of the Fiqa sequence was deposited during the final stages of the emplacement of the allochthonous units of Hawasina and Haybi complexes, and the Semail Ophiolite (Ali et al., 2008).

Upper Cretaceous and Tertiary Sequence

This sequence is characterised by highly deformed reflectors over the eastern part of the seismic profile. Internally, the sequence displays strong amplitude, continuous, parallel reflectors that can be mapped throughout the seismic section. The bottom section of the sequence is characterised by prominent high-amplitude, continuous reflector suggesting a conformable contact to the underlying Fiqa sequence. This is interpreted as a shallow-marine carbonate that was deposited as the margin subsided and was transgressed during the Maastrichtian. The lower parts of the sequence most likely represent the Simsima and Qahlah formations, respectively, and are exposed along the western flanks of northern Oman Mountains (Skelton et al., 1990; Noweir and Alsharhan, 2000; Osman, 2003; Searle and Ali, 2009). In the west, the thickness of this sequence is consistent throughout the seismic section and reaches approximately 1.4 sec TWTT, whereas to the east its thickness decreases dramatically due to uplift and erosion.

BACKSTRIPPING, SUBSIDENCE AND UPLIFT HISTORY, AND THERMAL HISTORY OF THE RIFTED MARGIN

Backstripping is a powerful tool for analysing the subsidence and uplift history of a sedimentary basin (e.g. Watts and Ryan, 1976). The procedure, which corrects the stratigraphic record for the effects of compaction, water depths, and sea-level changes (e.g. Steckler and Watts, 1978), determines the depth-to-basement in the absence of sediment and water loading. By comparing this depth to predictions of thermal models it is possible to constrain the amount of thinning, and hence heating of a margin during rifting.

We have backstripped biostratigraphic data from four exploration wells in the UAE foreland basin (Figures 5, 6 and 8). Two of the wells (W2 and W3) are located in the deep, flexed, part of the basin, about 80 km east of Abu Dhabi. The others are located to the east, near the thrust front (W1), and to the west, near the crest of the flexural bulge (W4).

Figure 6 shows the tectonic subsidence obtained by backstripping at well W2. The tectonic subsidence was computed assuming densities of water, sediment grains, and mantle of 1,030, 2,670, and 3,330 kg m^{-3}, respectively, and an Airy model of isostasy. Compaction was calculated using a porosity *versus* depth curve derived from the sonic velocity log (in the form of interval transit times) (Figure 7) following the method of Raiga-Clemenceau et al. (1988) and Issler (1992), which includes a provision for carbonates. The water depth is a more difficult problem. Whilst the rift margin sequences were deposited in a shallow-water carbonate shelf facies (< c. 20 m), the palaeobathymetry of the foreland basin sequence is unknown. We have therefore assumed a zero water depth for each stratigraphic sequence. Finally, the resulting tectonic subsidence and uplift were corrected for the effect of sea-level change using the smooth global curve of Watts and Steckler (1979), which has been shown by Miller et al. (2005) to be representative of the long-term, sea-level curve during the Mesozoic and Cenozoic.

Figure 6b shows that the sediment accumulation at well W2 can be divided into two parts: one represents the contribution of sediment and water loading, the other the unknown tectonic *driving* subsidence and uplift. The backstrip curve is characterised by a fast initial and then slowing subsidence. The curve shape resembles the typical concave-up profile of a rifted basin and so we interpret it as representative of the syn-rift and post-rift subsidence and uplift of the rifted margin that underlies the UAE foreland basin. At ca. 80 Ma, however, we see a significant increase in the subsidence, which we attribute to flexure following the emplacement of the Semail Ophiolite on the margin. The subsidence then slows and at ca. 25–15 Ma there is another increase, which we attribute to the collision of the Arabian and Eurasian plates.

The main features in the backstrip curve at well W2 are repeated at the nearby well W3 (Figure 8a). This reassures us that we have corrected the stratigraphic record at each well for local effects and that backstripping does indeed isolate the main features of the regional tectonic subsidence and uplift. The curve at well W1 (Figure 8b) is interesting because it contains a repeat sequence since it penetrated the Oman Mountains thrust front. There is a suggestion from the backstrip curves that the

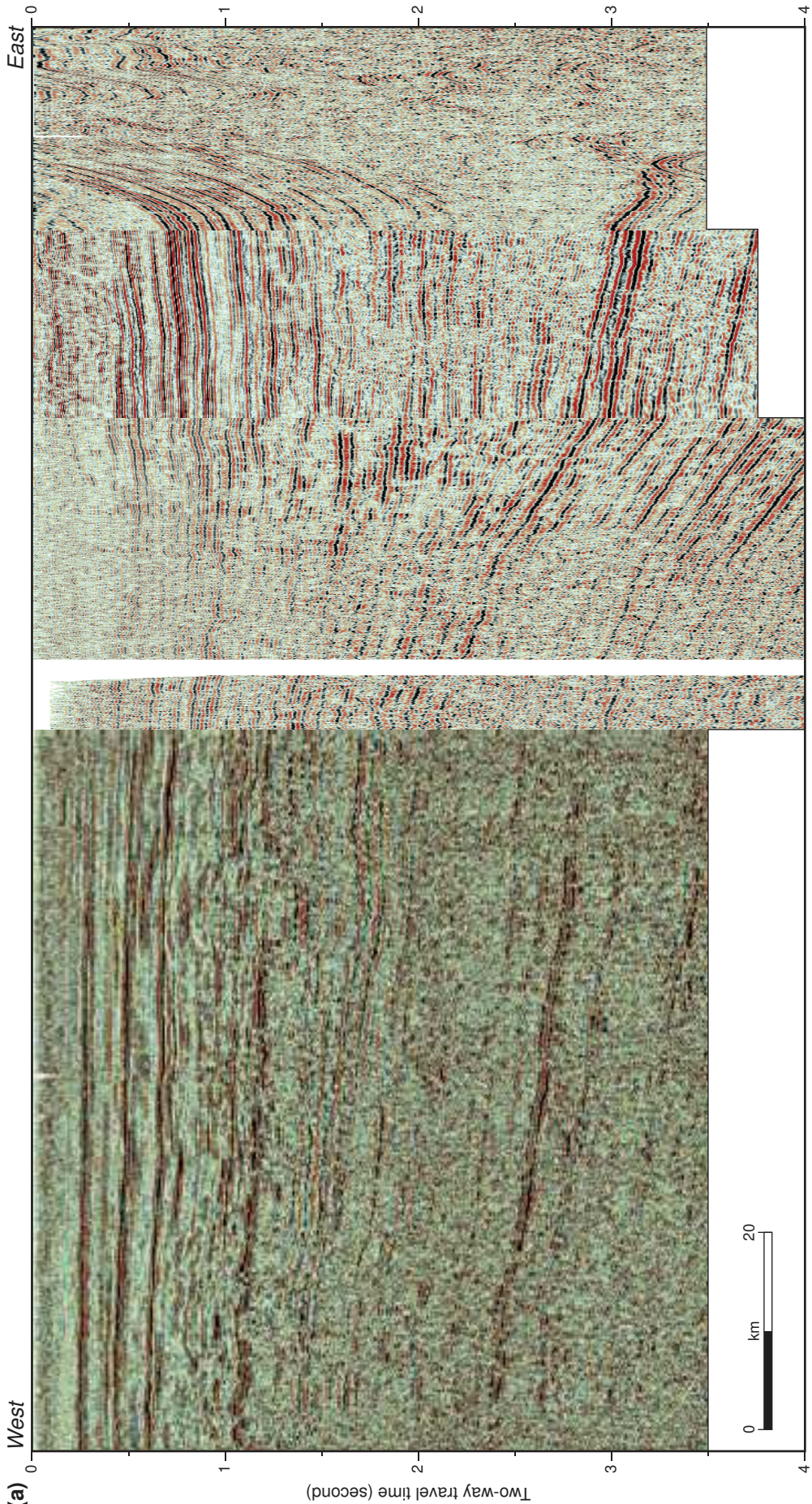

Figure 4a: Uninterpreted composite regional seismic reflection profile across the UAE foreland basin (for location see Figure 1).

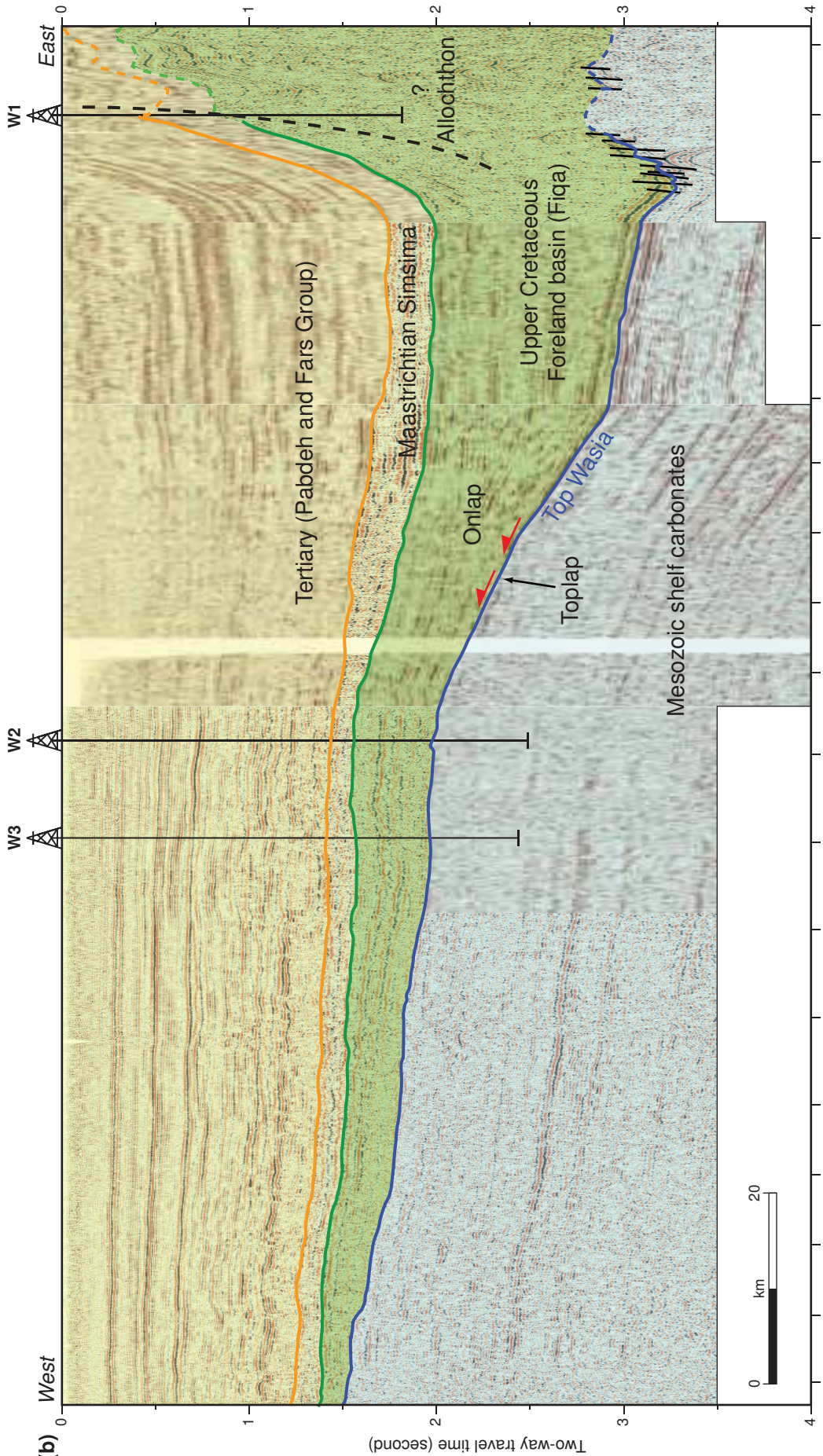

Figure 4b: Interpreted seismic reflection profile showing the UAE foreland basin and the underlying rifted margin sequences. Note the progressive onlap of the Fiqa on the Mesozoic shelf carbonates, which delineates the transition from an extensional rifted margin setting to a compressional foreland basin setting. The exploratory wells, W1, W2 and W3 are shown along the profile.

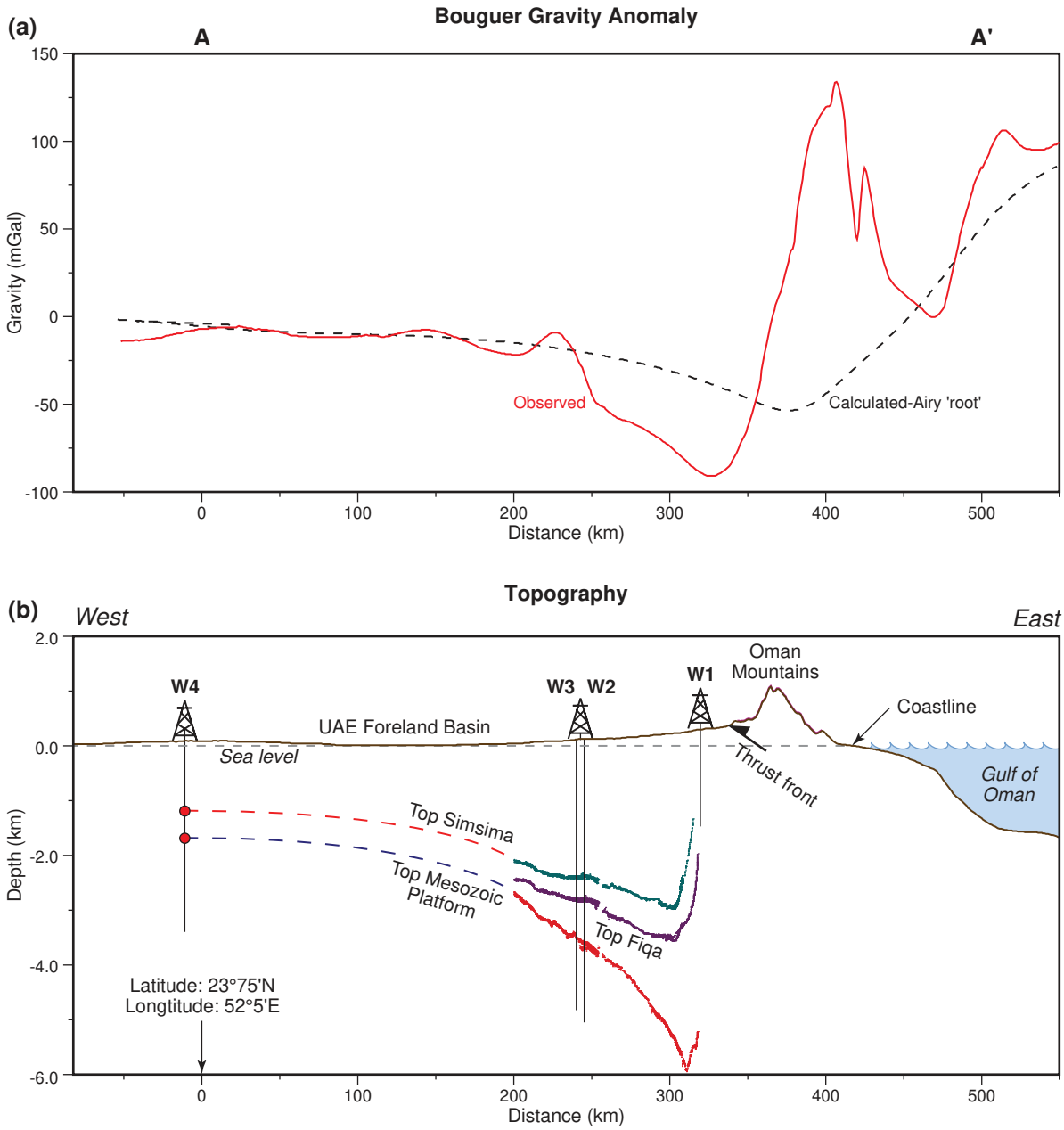

Figure 5: Bouguer gravity anomaly and topography profile along Profile AA′. The wells W1, W2, W3 and W4 have been projected orthogonally onto the profile.

(a) Bouguer gravity anomaly. Red line represents the observed. Dashed black line is the calculated gravity effect of the compensation of the topography based on the Airy model.

(b) Topography. The green, purple, and red-filled dots show the depth converted Two-Way Travel Time (TWTT) picks to the top of the Simsima, Fiqa, and top of the Mesozoic platform, respectively.

increase in tectonic subsidence at ca. 80 Ma is greater in well W1 than it is in well W2. This result is not unexpected because well W1 is located nearer to the ophiolite load than well W2. Well W4 (Figure 8c), however, is located further away and therefore the ophiolite-induced increase in subsidence is less apparent at this well.

We compare in Figure 9 the tectonic subsidence and uplift at well W3 to predictions of a uniform stretching model (McKenzie, 1978) with different values of the amount of crust and mantle stretching, β. We use here a modified form of the McKenzie model (Cochran, 1981), which incorporates the effects of a finite duration of rifting. We assumed a rifting duration of 40 My and an initial crustal thickness, T_c, of 31.2 km. Furthermore, we moved the observed curves vertically until a satisfactory fit with the

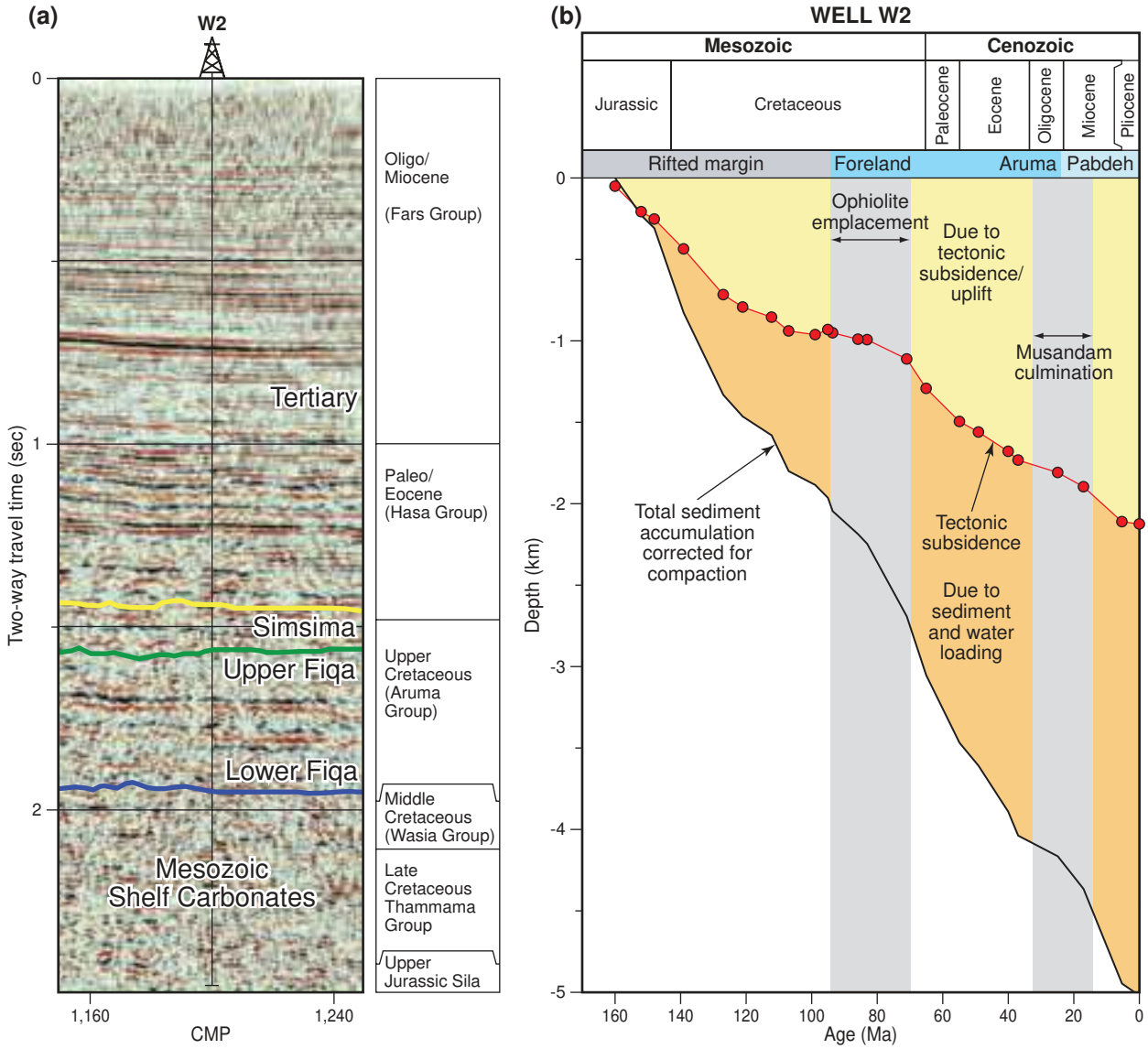

Figure 6: (a) Seismic reflection profile in the immediate vicinity of the well W2 showing well-to-seismic tie.

(b) Backstripping of biostratigraphic data from well W2 showing the total sediment accumulation at the well together with the backstripped tectonic subsidence and uplift. Note that the early part of the backstrip is concave-up and resembles the tectonic subsidence curves of rifted margins. We interpret the inflection points at ca. 80 Ma and ca. 25 Ma as due to orogenic loading.

modelled curves was achieved. This takes into account the fact that well W3, like the other wells, did not penetrate the syn-rift sediments. The best fit was for $\beta = 2.5$, which implies a thinning of the crust from 31.2 km before rifting to 12.5 km after.

The problem with such a large amount of thinning is that it is difficult to explain the *increase* that is observed (c. 75–125 mGal, Figure 5a) in the long-wavelength, regional, Bouguer gravity anomaly between the UAE foreland and the Gulf of Oman margin. The increase suggests that the Moho must be c. 5 km deeper beneath the UAE foreland than it is beneath the Oman margin. Indeed, an Airy model in which the depth to Moho decreases from 31.2 km beneath the foreland to 24.5 km beneath the Oman margin (a difference of c. 7 km) explains the observed regional increase reasonably well (dashed line, Figure 5a). If $\beta = 2.5$, as the model in Figure 9 suggests, then the depth-to-Moho beneath the UAE foreland would be 26.7 km (12.5 km + sediment fill). This is 2.2 km greater than beneath the Oman margin (24.5 km) and so would imply a change in the regional Bouguer anomaly between the UAE foreland and the Oman margin of 49 mGal, which is significantly less than the observed.

We therefore need to consider other ways of explaining the backstripped subsidence and uplift history that do not require such large amounts of thinning. One possibility is that the extension rather than being uniform varies with depth. For example, if there is more mantle extension than crustal extension at a particular locality then there would be less tectonic subsidence and, hence, crustal thinning.

Figure 10 shows that it is possible to explain the tectonic subsidence and uplift at well W3 with a depth-dependent extension model in which the amount of crustal extension, γ, is 1.3 and the amount of mantle extension, β, is 2.5. This parameter-pair explains the backstrip data well as can be seen from the sensitivity analysis in Figure 11a. Moreover, the smaller amount of crustal extension means a depth-to-Moho of 29.0 km (24.0 km + sediment fill) beneath the UAE foreland. This is 4.5 km greater than beneath the Oman margin (24.5 km) and so would imply a change in the regional Bouguer anomaly of 100 mGal. This explains the observed change well.

Figure 11a also shows that it is possible to fit the backstrip data at well W3 using other combinations of crust and mantle extension parameters. For example, γ = 2.3 and β = 1.5 fits the data as well as a γ of 1.3 and β of 2.5. However, this parameter pair implies a shallow Moho of 27.8 km (13.5 km + sediment fill) beneath the UAE foreland. This is 3.3 km greater than beneath the Oman margin and so would imply a change in the regional Bouguer anomaly of 73 mGal. This is slightly outside of the observed increase in the regional Bouguer gravity anomaly field.

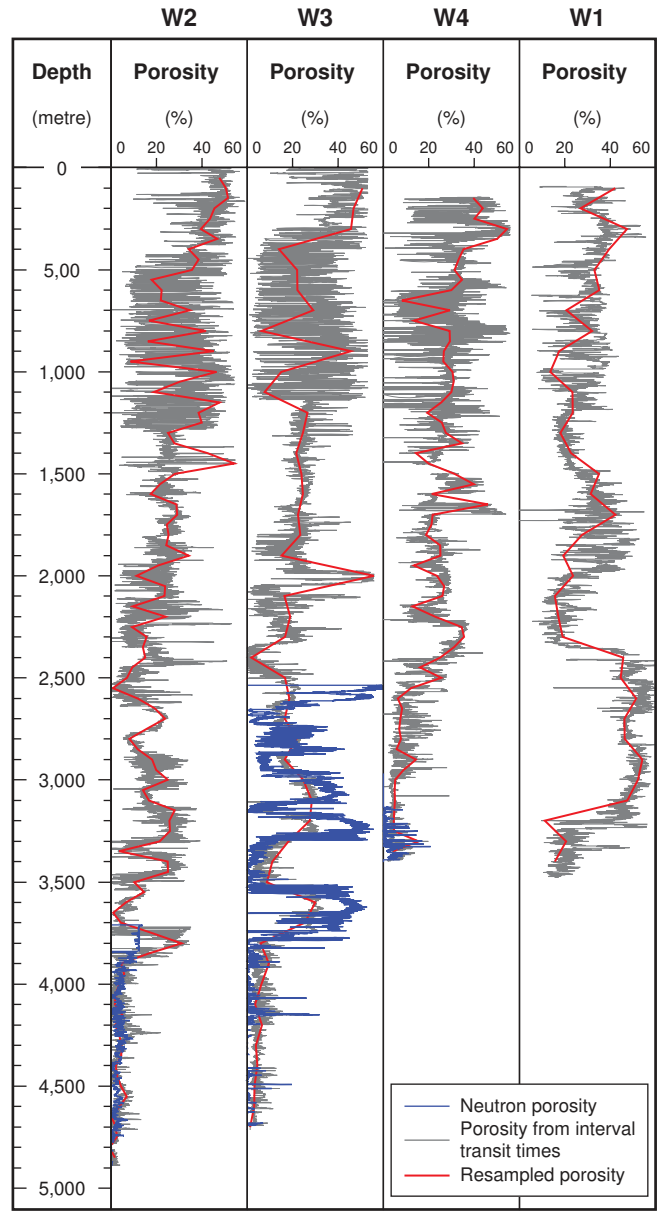

Figure 7: Porosity versus depth curves derived from sonic logs at wells W1, W2, W3 and W4. Also shown are resampled porosity and the neutron porosity in the reservoir zones. Note that the good match between the sonic-derived porosity and neutron porosity.

We caution, however, against the use of a depth-dependent extension model for only one margin of a conjugate margin pair. The total amount of extension in the crust and mantle across a conjugate margin pair must be equal. Otherwise, there would be a space problem (e.g. White and McKenzie, 1988). Unfortunately, we have no information on the subsidence and uplift history of the conjugate margin, which comprises the south-facing Neo-Tethyan rifted margin of the Central Iranian Plate and Lut Block.

OROGENIC LOADING

It is clear from the observed and calculated curves in Figures 9 and 10 that neither the uniform or depth-dependent extension models are able to explain all the features of the backstrip curves and the Bouguer gravity anomaly field. In particular, the models cannot account for the excess subsidence,

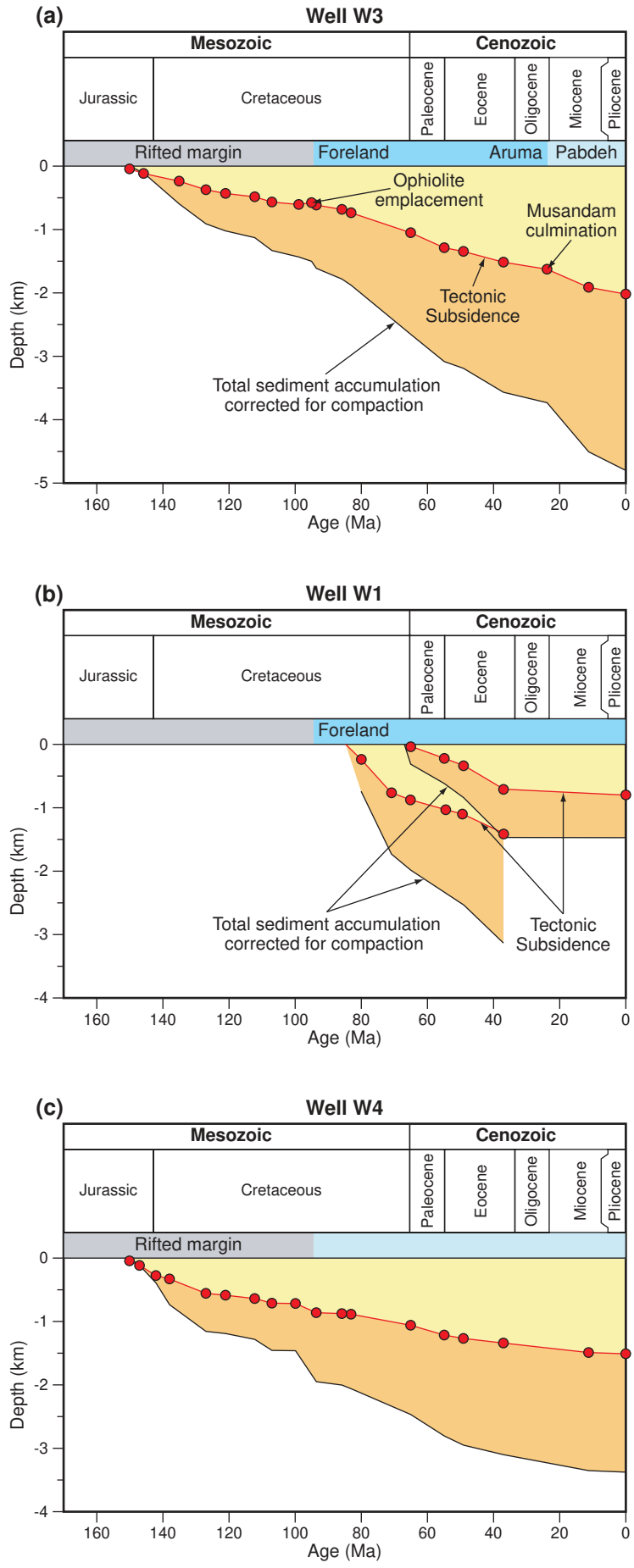

which begins at ca. 80–85 Ma and reaches a maximum value of c. 1 km at the present-day. Nor can they explain all the details of the Bouguer gravity anomaly, which shows a distinct short-wavelength gravity high-low 'couple' that is superimposed on the regional field. The initiation of the excess subsidence corresponds in time to the emplacement of the Semail Ophiolite and its associated thrusts. We therefore attribute the excess subsidence and the Bouguer gravity anomaly *couple* to orogenic loading associated with flexure of the underlying rifted margin.

In order to test this hypothesis, we have carried some forward flexure and gravity modelling, which takes into account all the loads, both surface and subsurface, that have been emplaced on the rifted margin since its formation. By comparing the calculated flexure and associated gravity anomalies due to these loads onto the observed base of the foreland sequence and the Bouguer gravity anomaly, we hope to constrain the effective elastic thickness, T_e, which is a proxy for the long-term strength of the rifted margin lithosphere.

Surface (Topographic) Loading

The present-day topography of northern Oman and the eastern UAE is made up of a number of thrusts and folds, which together constitute a load on the surface of the Arabian Plate. We have investigated the flexural effects and gravity anomaly of these loads and compared it to observations. The comparisons

Figure 8: Backstripping of biostratigraphic data from wells: (a) W3, (b) W1, and (c) W4. The concave-up rifted margin subsidence is visible in both wells W3 and W4. Note that the effects of orogenic loading are more clearly seen in well W1 than in wells W3 and W4 due to its proximity to the thrust front.

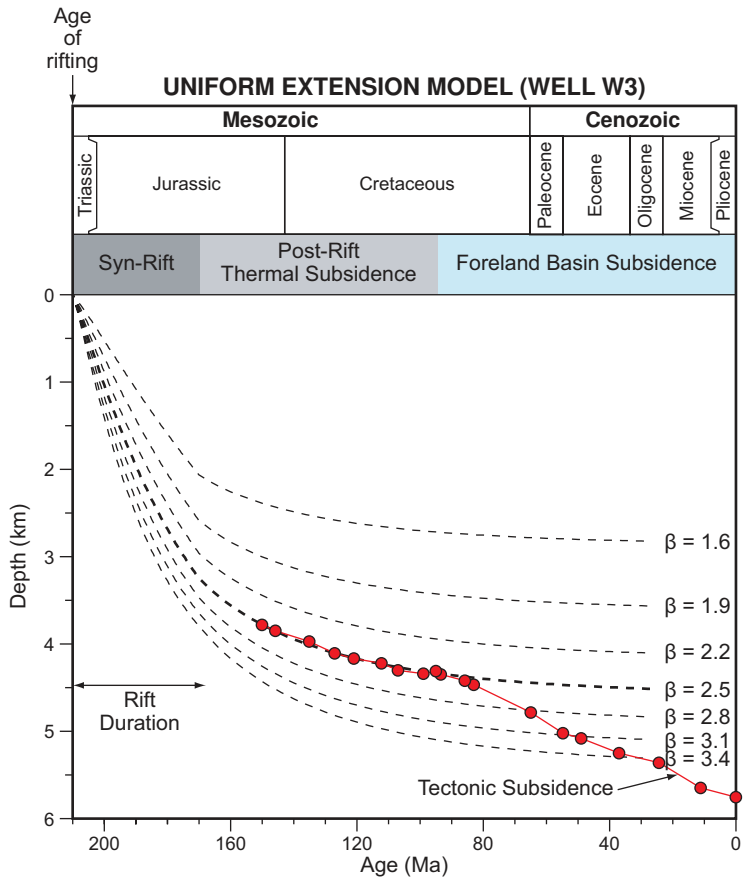

Figure 9: Comparison of the backstrip at well W3 to the predictions of a uniform extension model with crust and mantle extension, β, in the range 1.6–3.4. The calculated is based on a rift duration of 40 My and the thermal parameters in Table 1. The best fit between the early part of the tectonic subsidence curve and the calculated curve is for $\beta = 2.5$.

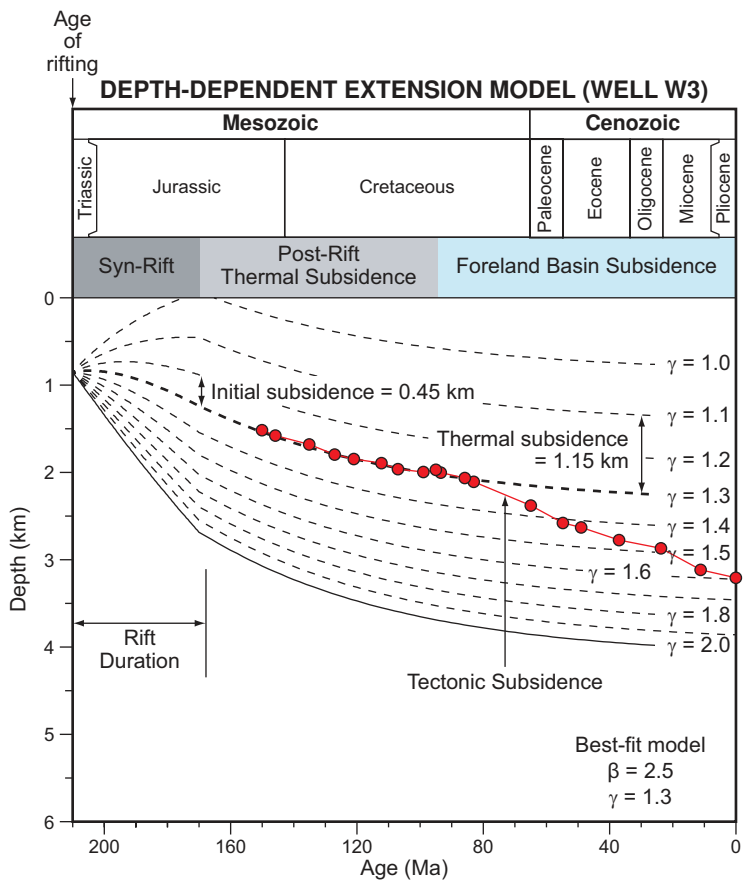

Figure 10: Comparison of the backstrip at well W3 to the predictions of a depth-dependent extension model with a mantle extension, β, of 2.5 and a crust extension, γ, in the range 1.0–2.0. The best fit is for $\gamma = 1.3$.

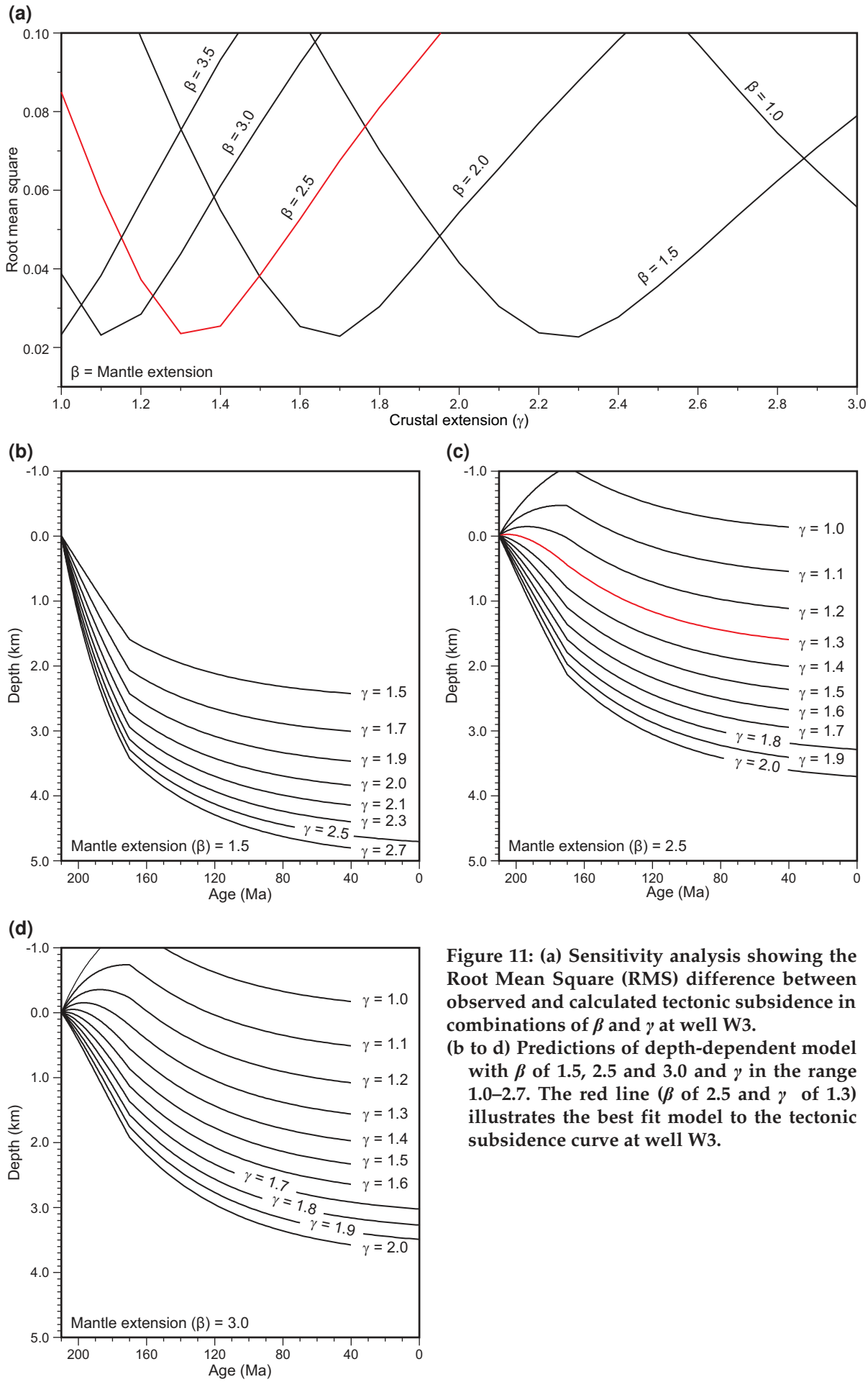

Figure 11: (a) Sensitivity analysis showing the Root Mean Square (RMS) difference between observed and calculated tectonic subsidence in combinations of *β* and *γ* at well W3.
(b to d) Predictions of depth-dependent model with *β* of 1.5, 2.5 and 3.0 and *γ* in the range 1.0–2.7. The red line (*β* of 2.5 and *γ* of 1.3) illustrates the best fit model to the tectonic subsidence curve at well W3.

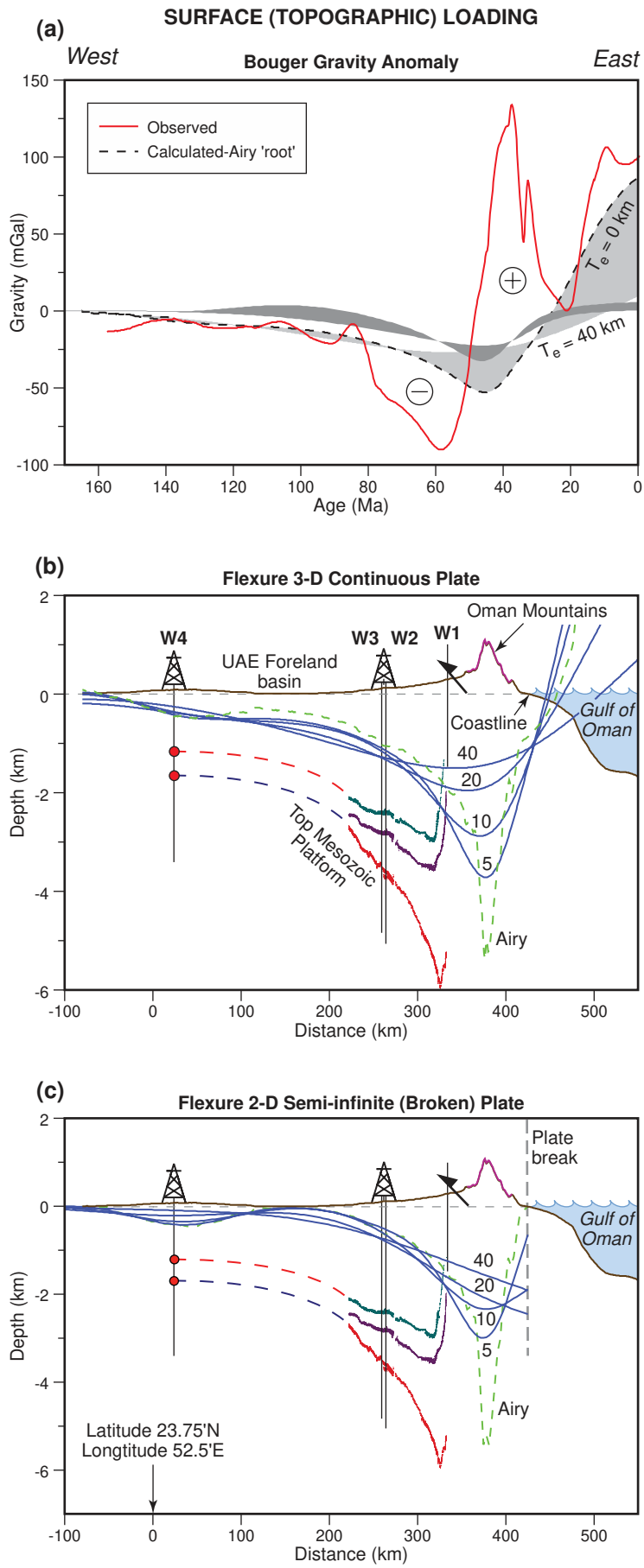

show (e.g. Figures 4 and 5) that the UAE foreland basin has been flexed downwards by up to 4 km, over horizontal distances of up to 250 km.

Figure 12 shows the calculated flexure and Bouguer gravity anomaly that would be expected along projected Profile AA′ (Figures 1 and 3) for surface (i.e. topographic) loading, using both continuous (Figure 12b) and semi-infinite (i.e. broken) (Figure 12c) elastic plates. The surface load is derived from a GEBCO (British Oceanographic Data Centre, 2003) 1 × 1 minute topography grid of the UAE and Oman and the flexure and gravity anomalies have been computed for a range of elastic thickness, T_e, values from 0 to 40 km. The solid blue lines show the flexure of a once undeformed, horizontal, surface at sea level. The largest amplitude and shortest wavelength of flexure is for T_e = 0 km, which corresponds to the predictions of an Airy model. The smallest amplitude and longest wavelength of flexure is for T_e = 40 km. Figures 12b and 12c show that the best overall fit to the

Figure 12: (a) Comparison of the observed Bouguer gravity anomalies and flexure along Profile AA′ to calculated Bouguer gravity anomalies and flexure based on surface (i.e. topographic) loading only. (b) 3-D continuous elastic plate models. (c) 2-D semi-infinite plate models. The magnitude of the surface load was estimated from the GEBCO grid. The comparisons show that while surface loading with T_e c. 5 km can explain the observed flexure of the top of the Mesozoic platform it is unable to explain the Bouguer gravity anomaly high over the eastern Oman Mountains and western UAE foreland basin. This conclusion is robust and is not dependent on whether we have used a 3-D continuous elastic plate or a 2-D semi-infinite plate in the flexure calculations.

top of the flexed Mesozoic carbonate platform is for T_e c. 5 km. This T_e appears to explain both the amplitude and wavelength of the observed flexure.

We note that all the calculated flexure curves in Figures 12b and 12c are offset vertically from the top of the Mesozoic platform. This offset is attributed to the fact that the foreland basin is overfilled such that the flexural bulge is obscured beneath Abu Dhabi by approximately upto 2 km of Upper Cretaceous and younger sediment. We are not certain about the origin of the accommodation space required to explain this excess sediment thickness, but we believe that it might be related to the present-day, northerly subduction of the oceanic crust of the Gulf of Oman (Neo-Tethys Ocean) beneath Eurasia in the region of the Zagros-Makran syntaxis.

While surface loading can therefore explain the shape of the observed flexure, it is unable to account for the Bouguer gravity anomaly *couple* that is observed over the Oman Mountains and flanking UAE foreland. This is well seen in Figure 12a, which shows the calculated gravity anomaly for surface loading of both a continuous (light grey shade) and semi-infinite (i.e. broken) (dark grey shade) elastic plate and $0 < T_e < 40$ km. The calculated anomalies show the same overall pattern: a *low* over the region of highest topography and a *high* that increases towards the Oman margin. None of the calculated curves are able to explain, however, the observed *high*, which reaches its maximum value of c. 100 mGal east of the peak topography, or the observed low of c. 50 mGal, which reaches its minimum value in the vicinity of the main thrust front. The high correlates with an outcrop of ophiolite while the low correlates with the deepest part of the UAE foreland basin. We therefore attribute the high-low Bouguer gravity anomaly *couple* to an additional, subsurface, ophiolite load and its associated flexure.

Buried (Ophiolite) Loading

Geological studies suggest that Semail Ophiolite emplacement has occurred through the obduction of oceanic crust and mantle rocks onto the leading edge of the Neo-Tethyan rifted margin (e.g. Glennie et al., 1973; Tilton et al., 1981; Lippard et al., 1986; Searle and Cox, 1999; Warren et al., 2003). The oceanic crust and mantle was probably generated above an intra-oceanic, east-dipping subduction zone by sea-floor spreading behind an island arc deep-sea trench system.

Figure 13 shows a simple model for the flexure and gravity anomaly that would result from buried (ophiolite) loading. The load is assumed to move across the surface of the crust by thrusting. As it moves, the load flexes the crust beneath and in front of it. We assume that the flexure fills with water and that any sediment that displaces the water further loads and flexes the crust and mantle. The corresponding gravity anomaly reflects both the loads and the resulting flexure. The calculated gravity anomaly curve shows that ophiolite loading is associated with a large-amplitude positive gravity anomaly that is flanked on one side by a small-amplitude negative anomaly. Sediment loading reduces the amplitude of these anomalies because it is associated with a positive anomaly over the maximum sediment thickness (sediments have a higher density than water) and a low in flanking regions.

We have applied this simple buried-loading model to the seismic and gravity anomaly data acquired along the projected Profile AA′ (Figures 1 and 3). As a first step, we estimated the magnitude of the ophiolite load by calculating the difference between the observed Bouguer anomaly and the calculated anomaly based on surface loading anomaly. We then used the positive part of the difference, together with the Bouguer slab formula, to compute the equivalent height of the buried load for an assumed density contrast between the ophiolite and the displaced material. This load was then placed onto the surface of an elastic plate and subsequently, the flexure and gravity anomalies calculated in the same way as for surface loading.

Figures 14a to 14e show the steps in the gravity anomaly (left-hand panel) and flexure (right-hand panel) calculations assuming T_e = 25 km. The other model parameters are as listed in Table 1. The contribution from crustal thinning (Figure 14d) has been calculated by applying an Airy model for the compensation of the topography. Figure 14e shows the sum of the gravity anomaly and flexure due to surface and buried loading, sediment loading, and crustal thinning, which can be compared to the observed Bouguer anomaly and the flexure of the top of the Mesozoic platform.

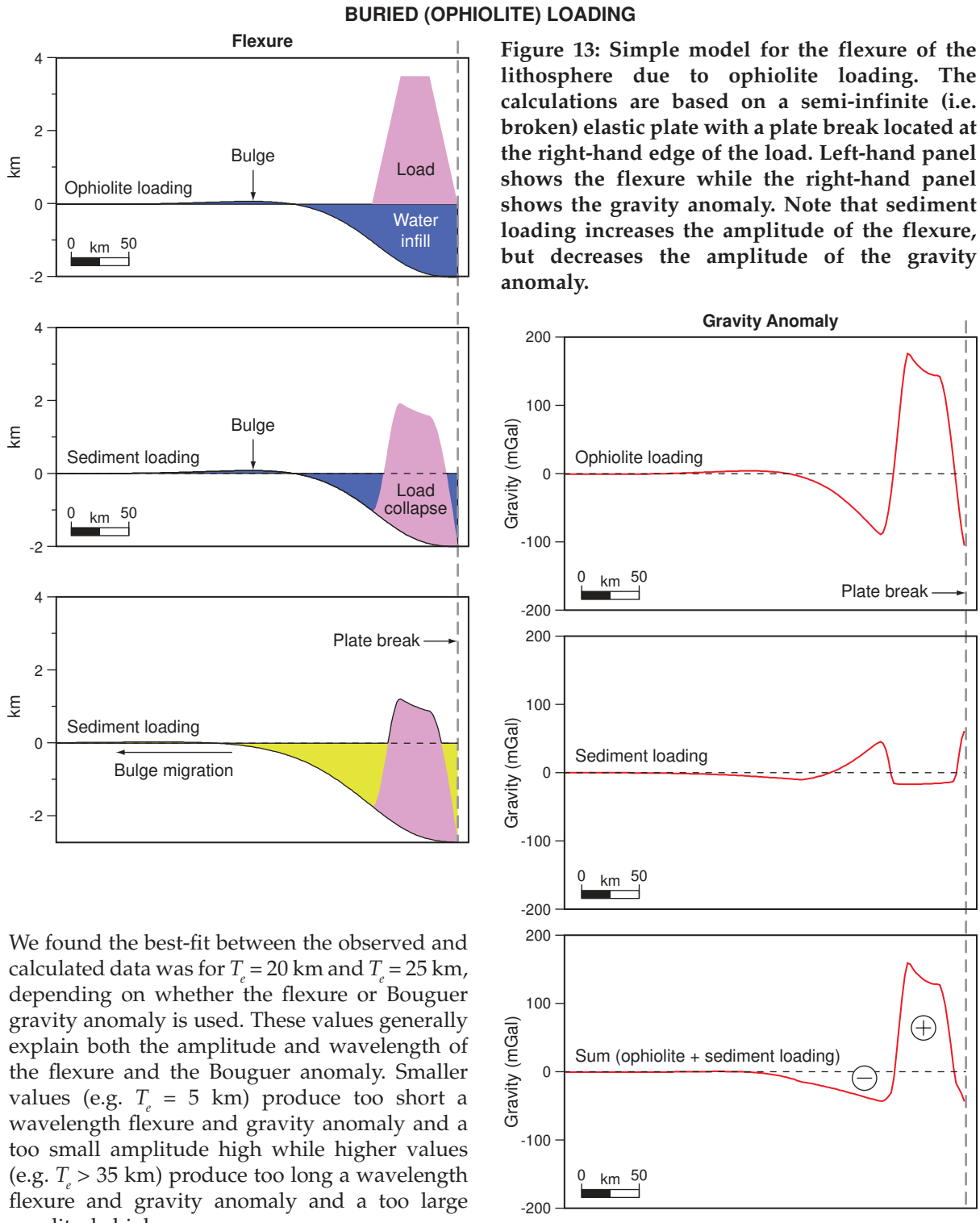

Figure 13: Simple model for the flexure of the lithosphere due to ophiolite loading. The calculations are based on a semi-infinite (i.e. broken) elastic plate with a plate break located at the right-hand edge of the load. Left-hand panel shows the flexure while the right-hand panel shows the gravity anomaly. Note that sediment loading increases the amplitude of the flexure, but decreases the amplitude of the gravity anomaly.

We found the best-fit between the observed and calculated data was for $T_e = 20$ km and $T_e = 25$ km, depending on whether the flexure or Bouguer gravity anomaly is used. These values generally explain both the amplitude and wavelength of the flexure and the Bouguer anomaly. Smaller values (e.g. T_e = 5 km) produce too short a wavelength flexure and gravity anomaly and a too small amplitude high while higher values (e.g. $T_e > 35$ km) produce too long a wavelength flexure and gravity anomaly and a too large amplitude high.

DISCUSSION

Sediment Thickness and Crustal Structure

The results of our thermal and gravity studies have implications for the sediment thickness and crustal structure of the UAE foreland basin and the Oman Mountains. Figure 15 compares, for example, the crustal structure inferred from the thermal modelling at well W3 with the structure deduced from flexure and gravity modelling of both surface and subsurface (i.e. buried) loads.

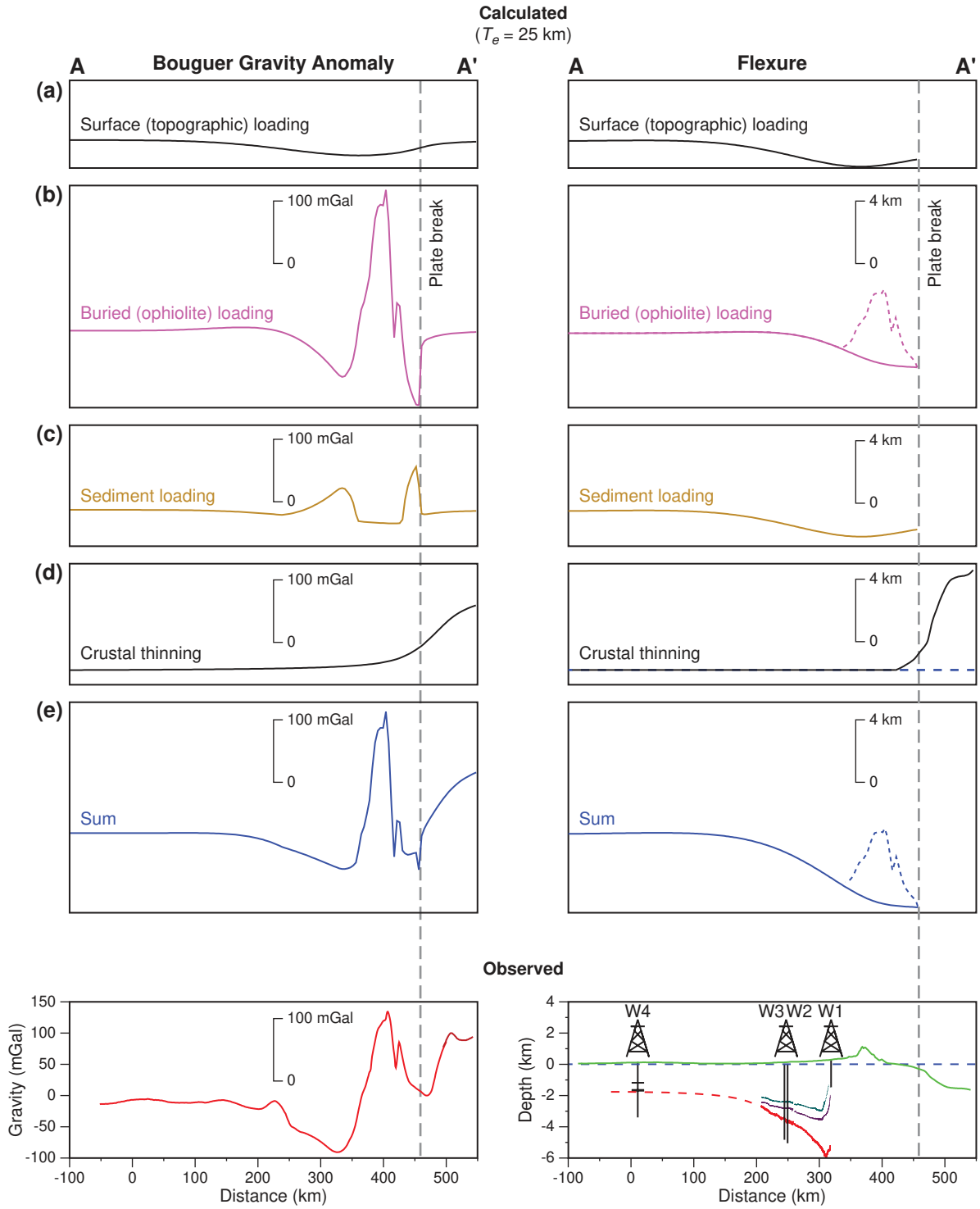

Figure 14: Comparison of the observed Bouguer gravity anomalies and flexure along Profile AA′ to calculated Bouguer gravity anomalies and flexure based on combined surface and subsurface (i.e. buried) loading of a semi-infinite (i.e. broken) elastic plate. The plate break was assumed to be located 40 km oceanward of the coastline. The magnitude of the buried load was estimated from the difference between the observed Bouguer gravity anomaly high and the calculated gravity effect of an Airy "root" (i.e. the dashed black line in Figure 12a). The comparisons show that a combined loading model with T_e c. 25 km can explain both the flexure of the top of the Mesozoic platform and the Bouguer gravity anomaly high and flanking low. Left-hand panel shows the Bouguer gravity anomaly while the right-hand panel shows the flexure.

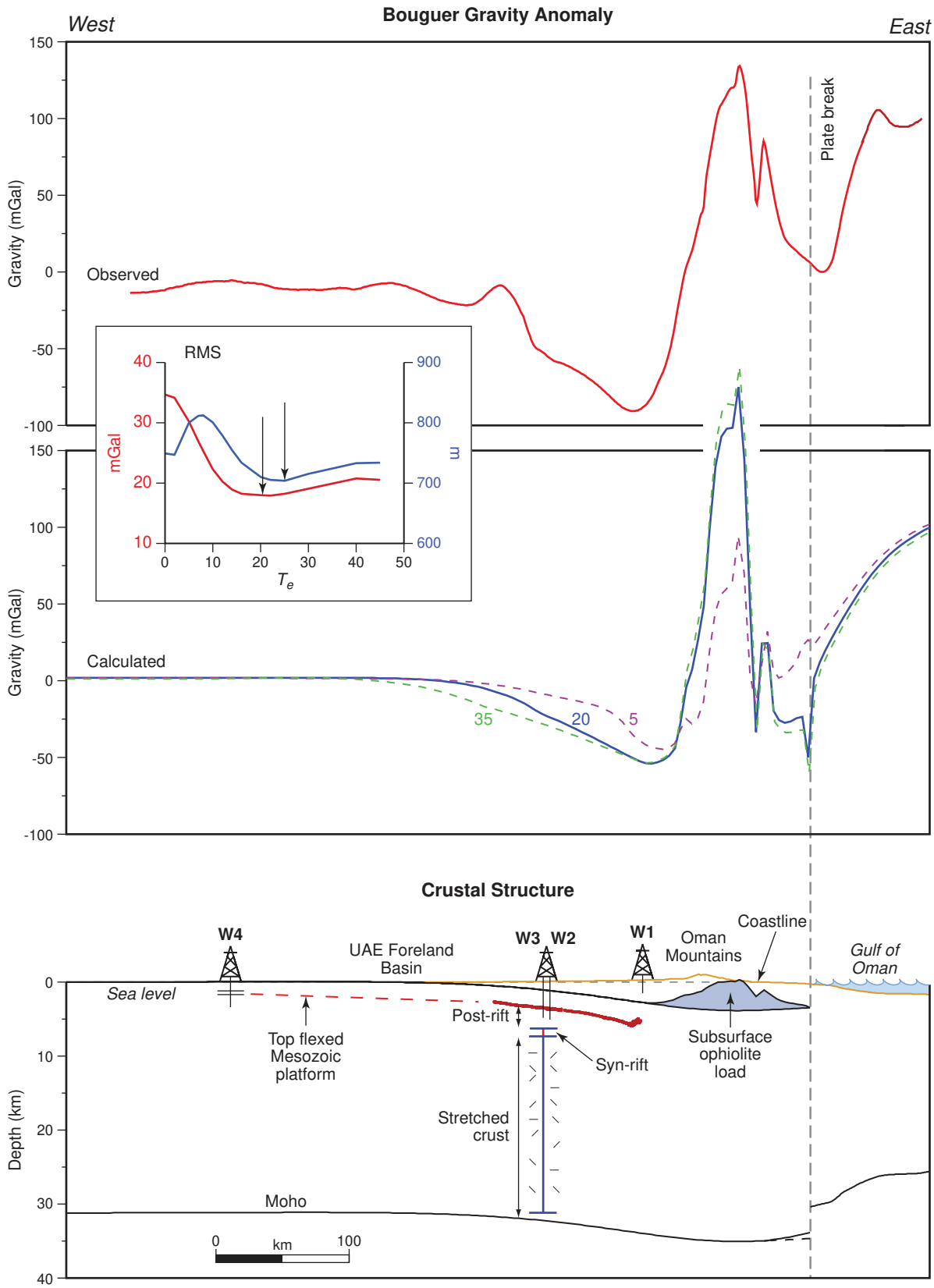

Figure 15: Crustal structure implied by the combined surface and buried loading model in Figure 14. Note that the crust is expected to be thinner than normal beneath the UAE foreland basin because of rifting and thicker than normal beneath the Oman Mountains because of ophiolite loading and flexure. The inset shows the RMS difference between observed and calculated gravity anomalies (red line) and the top of the flexed Mesozoic platform (blue line).

The initial and thermal subsidence inferred by our best-fit thermal model at W3 (Figure 10) implies, using the densities in Table 1, a thickness of syn-rift and post-rift sediments of 1.4 km and 3.6 km, respectively, at the well site. The best-fit model also implies a crustal thickness of 24 km. The depth-to-Moho at the well site is the sum of the foreland basin sequence, the rifted margin sequence, and the crustal thickness, which gives 32.4 km (3.4 + 3.6 + 1.4 + 24.0) as illustrated in Figure 15. This agrees well with the predicted depths based on surface and buried loading. Since well W3 terminated at a depth of c. 4.8 km, then the best-fit model suggests that well W3 only penetrated less than half of the post-rift sequence.

Figure 15 also shows that the Moho deepens to c. 35 km beneath the Oman Mountains and then thins towards the Gulf of Oman. We attribute the deepening to flexure due to surface (i.e. topographic) and buried loading, and the thinning to transitional crust between continental and oceanic crust.

We caution that our estimates of Moho depth are based on an assumption of an initial crustal thickness and zero elevation crustal thickness of 31.2 km (e.g. Table 1). Larger or smaller values will mean we may have overestimated or underestimated Moho depths, respectively.

Table 1
Summary of parameters used in the thermal and mechanical modelling

Parameter	Value
Density of surface load (i.e. topography)	2,800 kg m^{-3}
Density of subsurface (ophiolite) load	3,100 kg m^{-3}
Density of material displaced by ophiolite	1,030 kg m^{-3}
Density of sediment	2,600 kg m^{-3}
Density of material displaced by sediment	1,030 kg m^{-3}
Density of crust	2,800 kg m^{-3}
Density of mantle	3,330 kg m^{-3}
Thickness of zero elevation crust	31.2 km
Young's Modulus	100 GPa
Poissons Ratio	0.25
Thermal thickness of the lithosphere	125 km
Temperature at base of lithosphere	1,330 °C
Coefficient of volume expansion	3.28 x 10^{-5} ºC^{-1}
Thermal diffusivity	8.0 x 10^{-7} m^2 s^{-1}
Thermal conductivity of water	0.63 W °C^{-1} m^{-1}
Thermal conductivity of sediment grains	2.09 W ºC^{-1} m^{-1}
Density of sediment grains	2,650 kg m^{-3}

Unfortunately, there are only a few seismically constrained estimates of Moho depths in the UAE and Oman region. Al-Lazki et al. (2002), Al-Damegh et al. (2005) and Hansen et al. (2007) suggest c. 40 km beneath the Oman foreland, c. 50 km beneath Al Jabal al-Akhdar, and c. 35 km beneath the Oman coast. However, these estimates are based on receiver functions, which do not have the precision of controlled-source seismic refraction surveys. There have been several long seismic reflection profiles acquired over the northern UAE foreland and Oman Mountains (Figure 1) (Roure et al., 2006). The western part of these profiles in the foreland shows prominent bright reflections at 15 sec TWTT, which are interpreted as the Moho at c. 44 km depth beneath a layered lower crust. However, the velocity structure of the crust that underlies the sediments is difficult to determine from semblance analysis and so this needs to be considered as only an approximate estimate of the Moho depth.

We have tested the effects of a thicker crustal thickness on our thermal model by calculating the RMS (Root Mean Square) difference between observed and calculated tectonic subsidence and uplift for a range of γ and β values at well W3. Figure 16 shows that if the thickness is increased to 40 km, the best-fitting values of the crustal extension shifts from 1.3 to 1.7–2.0. This increases the amount of crustal thinning, however, and therefore makes it more difficult to explain the regional gravity field.

Effective Elastic Thickness (T_e) Versus Age (Ma)

The T_e that we have estimated from the flexure of the top of the Mesozoic platform and the Bouguer gravity anomaly describes the overall 'architecture' of the UAE foreland basin. Its main significance, however, is that it reflects the long-term thermal and mechanical properties of the underlying Neo-Tethyan rifted margin some 80 My following the end of rifting. We can therefore compare it to other rifted margins, especially ones that have also had large, discrete, loads imposed on them.

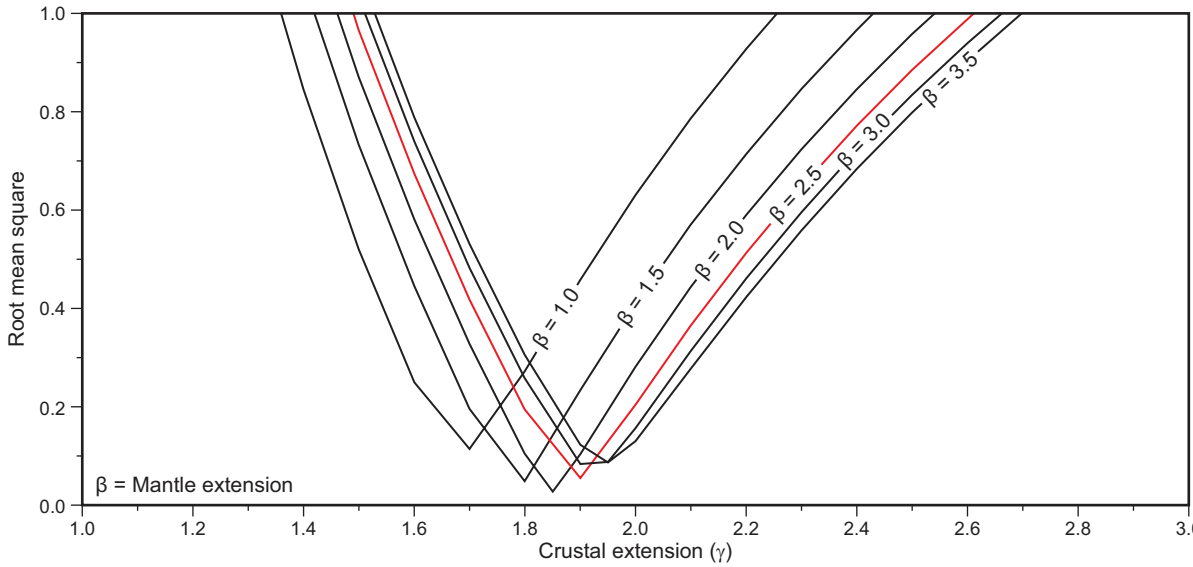

Figure 16: RMS difference between observed and calculated tectonic subsidence for a range of γ and β values at well W3 with initial crustal thickness of 40 km. The figure shows that the best fitting values of the crustal extension increase from 1.3 (Figure 11) to 1.7–2.0.

Figure 17 shows a compilation of T_e estimates from rifted margins that were subject at some stage during their evolution to a large discreet load. They include the South China Sea margin, which rifted about 50–60 Ma and was loaded by thrusts and folds in Taiwan during the Late Miocene – Early Pliocene (Lin and Watts, 2002), and the NE Brazil margin, which rifted ca. 120 Ma and was loaded by the Amazon fan in the Middle – Late Miocene (Rodger et al., 2006). The plot suggests a relationship between T_e and age since rifting. Margins that were loaded soon after the end of rifting (e.g. the South China Sea) have low values and, hence, are weak, while margins loaded over a long time after the end of rifting (e.g. NE Brazil) have high values and, hence, are strong. The Neo-Tethyan margin that underlies the UAE foreland basin is apparently an intermediate case in which the lithosphere is neither weak nor strong. We note also from Figure 17 that the T_e values are quite well described by the depth to the 450° C isotherm based on the cooling plate model (Parsons and Sclater, 1977), suggesting that rifted margins are weak early on (i.e. during the syn-rift) because they are hot and strengthen later on (i.e. during the post-rift) as they cool.

These results have consequences for the rheological properties of stretched continental lithosphere. In particular, they suggest that like the oceanic lithosphere, continental lithosphere regains its strength following a heating event. Support for this suggestion has come from both Yield Strength Envelope (YSE) considerations (e.g. Perez-Gussinye et al., 2001) and numerical modelling (Burov and Poliakov, 2001) studies. The latter study shows that the multi-layer rheology, and hence T_e, structure of continental lithosphere has a major effect on the structural styles that develop during rifting.

Thermal and Maturation History

The UAE foreland basin is one of a number of sub-basins on the Arabian Plate that collectively form one of the world's largest repositories of oil and gas resources (Alsharhan, 1989; Alsharhan and Nairn, 2003). It is pertinent therefore to examine the implications of our subsidence history, gravity and flexure analysis for the thermal history of the basin.

We have shown that the early, concave-up, tectonic subsidence at well W3 can be best explained by a depth-dependent extension model with γ = 1.3 and β = 2.5. This parameter pair implies a certain amount of crust and lithosphere heating at the time of rifting and, hence heat flow as the basement cools. Thermal modelling using the parameters in Table 1 shows that the heat flow varies over time, rising from 33 mW m^{-2} at the start of rifting, to a peak of 52 mW m^{-2} soon after rifting and then decreasing steadily to its initial value.

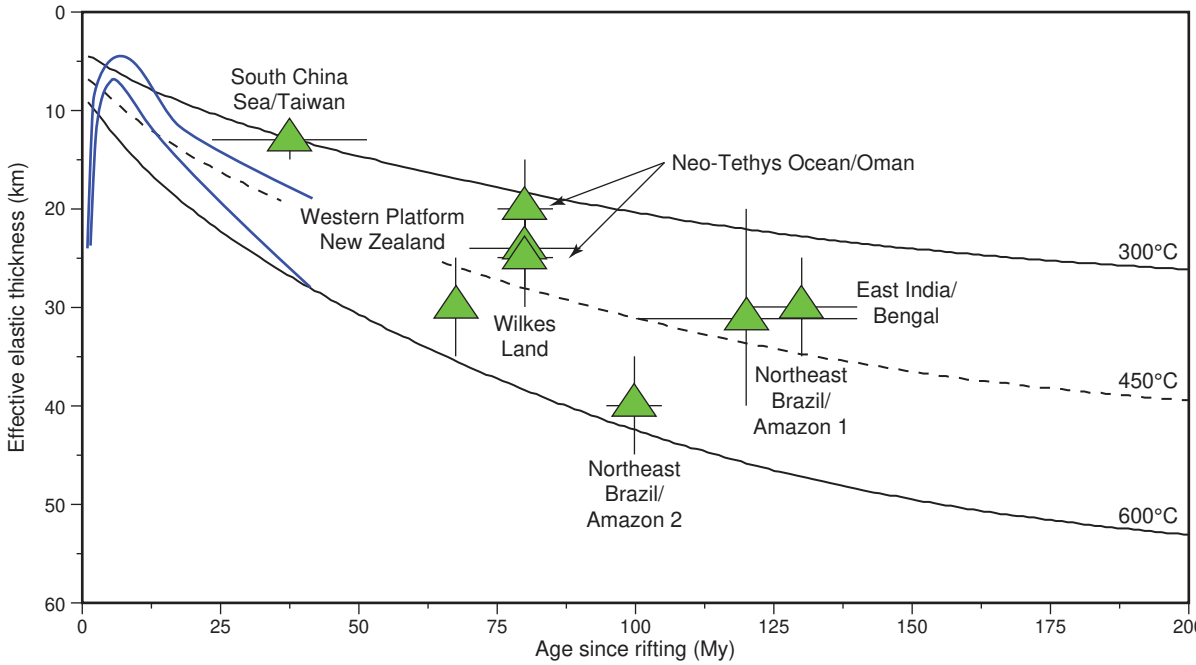

Figure 17: Plot of T_e versus age since the initiation of rifting for selected rifted margins, which were subject to unusually large loads during their evolution. The plot includes the NE Brazil (Rodger et al., 2006) and East India (Krishna et al., 2000) margins, which were loaded by large deep-sea fan systems of the Amazon River and Bay of Bengal, respectively, and the South China Sea (Lin and Watts, 2002) and Arabian Plate Tethyan (this paper) margins, which were loaded by orogenic loads in Taiwan and Oman, respectively. Also plotted are data from the Wilkes Land margin (Close et al., in preparation) and the Western platform, New Zealand (Holt and Stern, 1991). Thick blue lines show the predicted variation in T_e during and following rifting based on the numerical modelling of Burov and Poliakov, 2001.

We have used the basement heat flow to compute the temperature in the overlying sediments, assuming that the heat flow is the same in the cooling basement as it is in the sediments. The results suggest present-day (Figure 18a) temperatures of c. 130° C at the base of well W3. This agrees reasonably well with the observed bottom hole temperatures (150–163° C), especially when we take into account the high surface temperature (25° C) in the calculated temperatures.

We know from studies in different tectonic settings (e.g. Waples, 1980; Ungerer et al., 1990; Waples, 2002) that the maturation of hydrocarbons is a strong function of the time-temperature history. We have therefore used the temperature history in the UAE foreland to compute the Time-Temperature Index (TTI), which is a useful parameter with which to access the maturity of a particular source rock.

There are two main source rocks for petroleum generation in the UAE foreland. The first is the Diyab Formation (Oxfordian – Lower Kimmeridgian), which is the offshore equivalent of the Dukhan Formation. It is the major source for the Upper Jurassic (Arab Formation) and Lower Cretaceous (Thamama Group) reservoirs. The second is the Shilaif Formation (Upper Albian – Cenomanian). It is the main source for the Mishrif and Simsima reservoirs. Other minor source rocks include the Jilh, Uweinat, Shu'aiba (Bab Member) and Fiqa formations (Alsharhan, 1989).

Maturity estimations, based on vitrinite reflectance, indicate that the onset of oil generation in the Diyab and Dukhan formations began at 73 Ma and peaked in central, SW and NE onshore Abu Dhabi, at 56 Ma (Alsharhan, 1989; 1993a, b). In contrast, generation of oil in the Shilaif Formation started at 22.5 Ma and reached maximum oil generation at 3 Ma in central and NE of Abu Dhabi (Alsharhan, 1989).

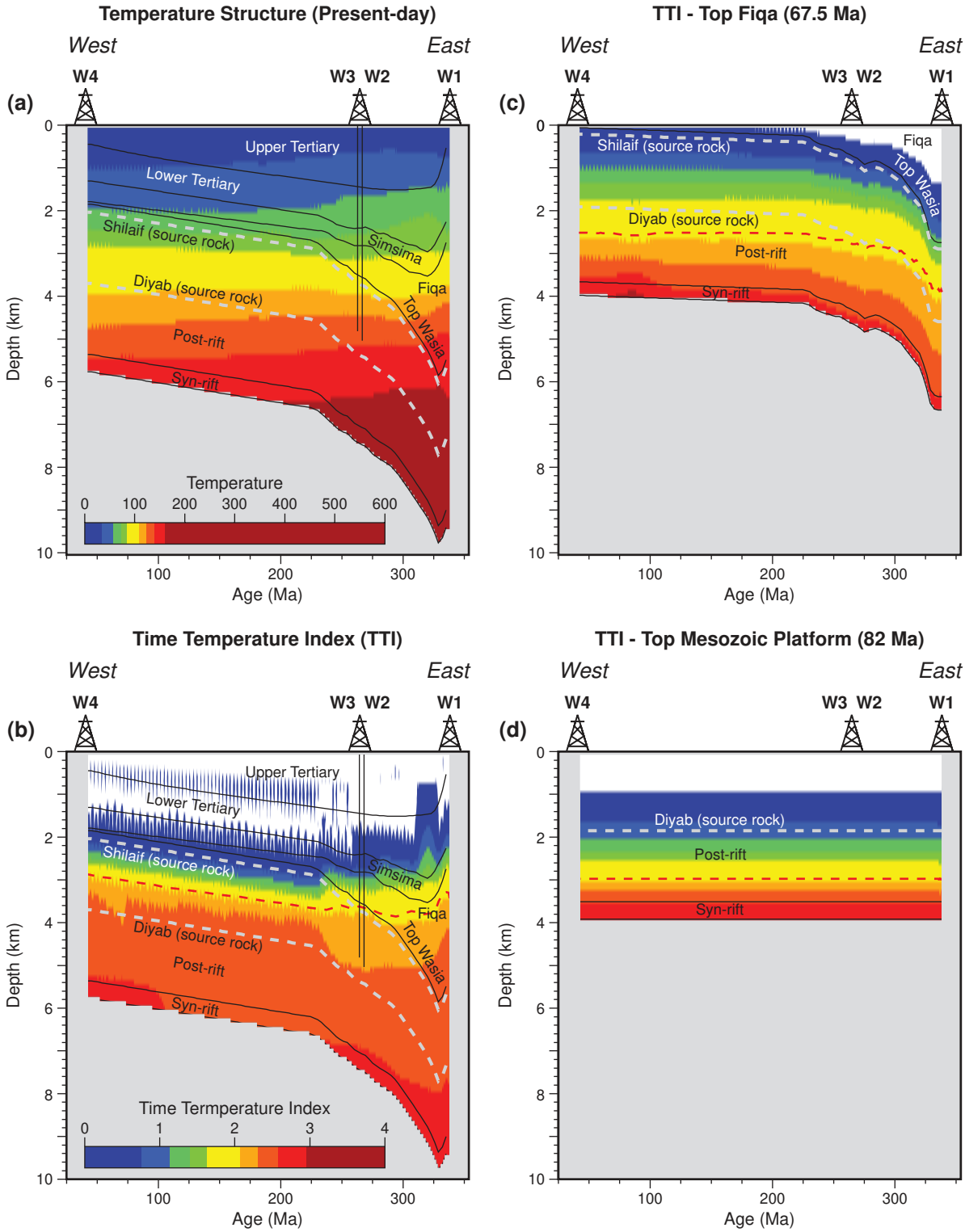

Figure 18: The thermal history of the UAE foreland basin. The post-rift sediment isopachs are based on the depth-converted seismic reflection profile data shown in Figure 4. The syn-rift isopach and the thermal history are based on the best-fit crust and mantle extension parameters derived from backstripping, crustal balancing and thermal modelling at well W3 (Figure 10). Other parameters are as listed in Table 1.

(a) Temperature structure at the present-day.

(b) The Time-Temperature Index (TTI) as defined by Wapples (1980). TTI = 2 is shown as a dashed red line and corresponds to peak oil generation.

(c) TTI at the top of Fiqa (ca. 67.5 Ma).

(d) TTI at the top of the Mesozoic platform (ca. 82 Ma). Thick dashed grey lines show the source rocks (Diyab and Shilaif).

Figures 18b, c and d show the TTI for the present-day, top Fiqa (ca. 67.5 Ma), and top Mesozoic platform (ca. 82 Ma), respectively. At the present time, the Diyab and Dukhan formations are highly to over-mature in most areas of the UAE. Whereas, the Shilaif is immature to early mature in the western onshore and offshore areas of the UAE, except in the eastern region where rapid subsidence in the foredeep area led to deeper burial. In this area the Shilaif is mostly either approaching the maximum oil generation phase or in the gas-condensate window, which is consistent with the condensate occurrences in Khusub, Margham and Sajaa fields along the western leading edge of the northern Oman Mountains.

Figures 18 also shows that the Upper Jurassic (i.e. middle part of the post-rift) did not reach maturity until ca. 67.5 Ma and then only in the deepest part of the basin, between wells W2 and W3 and well W1. The Upper Jurassic in the rest of the basin took longer and it is only by the present-day, that most of it became mature. This interpretation is consistent with the results of vitrinite reflectance, rock maturity and time of oil expulsion and burial history modelling of Upper Jurassic source rocks. For example, modelling of source rock maturity and time of oil expulsion in northeastern Saudi Arabia suggests that the Upper Jurassic source rocks reached maturity in Late Cretaceous ca. 75 Ma (i.e. Campanian) (Cole et al., 1994). Furthermore, similar results were obtained from geohistory analysis in a structurally deep part of eastern Saudi Arabia (Pollastro, 2003). These models show that the Jurassic source rocks are presently in the late stage of oil generation.

All the hydrocarbon accumulations in the UAE foreland occur in structural traps, although combined stratigraphic and structural or stratigraphic traps exist in some areas (Alsharhan, 1989). Major trap formation and modification are a result of the two main compressional events. The first, a Late Cretaceous phase (from the Late Cenomanian to the end of the Early Maastrichtian), during which obduction-related allochthonous thrust sheets of the Oman Mountains were emplaced from NE to SW onto the Arabian rifted margin. The second event, a Tertiary phase, is associated with the opening of the Red Sea and the collision of the Arabian and Eurasian plates, which started during Late Eocene and continues until the present-day (Searle et al., 1983; Searle, 1988b).

Our modelling results suggest that it was the first of these orogenic events and their accompanying loads and flexures that caused source rocks in the Upper Jurassic rifted margin sequence to reach maturity by the Late Cretaceous. Otherwise, it would have taken the sequence much longer to reach maturity with the consequence that hydrocarbons may not have been able to migrate into a suitable trap, even by the present-day.

CONCLUSIONS

We draw the following conclusions from this paper:

1. Seismic reflection profile and exploratory well data show that the UAE sedimentary basin can be divided into two main sequences: (1) a lower rifted margin sequence and (2) an upper foreland basin sequence. The margin sequence comprises at least 5 km of syn-rift and post-rift sediment. The foreland basin comprises at least 3.4 km of sediment. This yields a total sediment thickness of at least 8.4 km.
2. Backstripping of biostratigraphic data from four exploration wells suggest that the transition from an extensional rifted margin to a compressional foreland basin occurred ca. 80 Ma, which is within the range for the emplacement of the Semail Ophiolite.
3. The tectonic subsidence prior to 80 Ma is attributed to thermal contraction following heating and thinning of the crust at the time of rifting. The backstrip curves and the regional Bouguer gravity field are consistent with a model in which the margin developed by non-uniform depth extension and the mantle was extended by a greater amount than the crust.
4. The tectonic subsidence after 80 Ma is too large to be explained by a thermal contraction model. Gravity and flexure modelling suggest that the excess subsidence is caused by surface and subsurface ophiolite loading of a lithosphere with an effective elastic thickness (T_e) in the range of 20–25 km.
5. This T_e is similar to what would be expected if the rifted margin sequences loaded a lithosphere that increases its strength following heating at the time of rifting.

6. Thermal modelling suggests that Upper Jurassic post-rift source rocks would not normally be expected to reach maturity until the present-day. However, ophiolite loading and flexure increased the tectonic subsidence of the margin such that Upper Jurassic source rocks in the deepest part of the UAE foreland basin could have become mature as early as Upper Cretaceous.

ACKNOWLEDGEMENTS

We are grateful to The Petroleum Institute, Abu Dhabi, for its sponsorship of this project and ADNOC for the provision of the seismic reflection profile and well data used in this study, Tom Jordan and Melanie Savage for their help in acquiring gravity data in the field, and Mike Searle for many stimulating discussions on the tectonic evolution of the Oman Mountains. Two anonymous reviewers greatly improved the manuscript. The final design of the paper by Arnold Egdane is appreciated.

REFERENCES

Ali, M.Y., M. Sirat and J. Small 2008. Geophysical investigation of Al Jaww plain, eastern Abu Dhabi: Implications for structure and evolution of the frontal fold belts of Oman Mountains. GeoArabia, v. 13, no. 2, p. 91-118.

Al-Damegh, K., E. Sandvol and M. Barazangi 2005. Crustal structure of the Arabian Plate: New constraints from the analysis of teleseismic receiver functions. Earth and Planetary Sciences Letters, v. 231, p. 177-196.

Al-Lazki, A.I., D. Seber, E. Sandvol and M. Barazangi 2002. A crustal transect across the Oman Mountains on the eastern margin of Arabia. GeoArabia, v. 7, no. 1, p. 47-78.

Alsharhan, A.S. 1989. Petroleum geology of the United Arab Emirates. Journal of Petroleum Geology, v. 12, p. 253-288.

Alsharhan, A.S. 1993a. Asab field-United Arab Emirates Rub Al Khali Basin Abu Dhabi. In N.H. Foster and E.A. Beaumont (Eds.), Structural Traps VIII. Americal Association of Petroleum Geologists, Treatise of Petroleum Geology, Atlas of Oil and Gas Fields, p. 69-98.

Alsharhan, A.S. 1993b. Bu Hasa field-United Arab Emirates Rub Al Khali Basin Abu Dhabi. In N.H. Foster and E.A. Beaumont (Eds.), Structural Traps VIII. American Association of Petroleum Geologists, Treatise of Petroleum Geology, Atlas of Oil and Gas Fields, p. 99-127.

Alsharhan, A.S. and A.E.M. Nair 2003. Sedimentary basins and petroleum geology of the Middle East. Elsevier, p. 575-597.

Béchennec, F., J. LeMetour, D. Rabu, C.H. Bourdillon-de-Grissac, P. DeWever, M. Beurrier and M. Villey 1990. The Hawasina nappes: Stratigraphy, palaeogeography and structural evolution of a fragment of the south Tethyan passive continental margin. In A.F.H. Robertson, M.P. Searle and A.C. Ries (Eds.), The Geology and Tectonics of the Oman Region. Geological Society of London, Special Publication no. 49, p. 213-223.

Boote, D.R.D., D. Mou and R.I. Waite 1990. Structural evolution of the Suneinah Foreland, Central Oman Mountains. In A.H.F. Robertson, M.P. Searle and A.C. Ries (Eds.), The Geology and Tectonics of the Oman Region. Geological Society of London, Special Publication no. 49, p. 397-418.

British Oceanographic Data Centre 2003. The GEBCO Digital Atlas, Centenary Edition (CD-ROM), Liverpool.

Burgess, P.M. and L.N. Moresi 1999. Modelling rates and distribution of subsidence due to dynamic topography over subducting slabs: Is it possible to identify dynamic topography from ancient strata? Basin Research, v. 11, p. 305-314.

Burov, E. and A. Poliakov 2001. Erosion and rheology controls on synrift and postrift evolution: Verifying old and new ideas using a fully coupled numerical model. Journal of Geophysical Research, v. 106, p. 16,461-416,481.

Cochran, J.R. 1981. Simple models of diffuse extension and the pre-seafloor spreading development of the continental margin of the northwestern Gulf of Alden. Proceedings of the 26th International Congress Symposium on Continental Margins, Oceanologica Acta, p. 154-165.

Cole, G.A., M.J. Carrigan, H.H. Colling, H.I. Halpern, M.R. Khadhrawi and P.J. Jones 1994. Organic geochemistry of the of the Jurassic petroleum system in Eastern Saudi Arabia. In A.F. Embary, B. Beauchamo and D.J. Closs (Eds.), Pangea, Global Environments and Resources. Canadian Society of Petroleum Geologists, Memoir 17, p. 413-438.

Corfield, R.I., A.B. Watts and M.P. Searle 2005. Subsidence of the North Indian Continental Margin, Zanskar Himalaya, NW India. Journal of the Geological Society of London, v. 162, p. 135-146.

DeCelles, P.G. and K.A. Giles 1996. Foreland basin systems. Basin Research, v. 8, p. 105-123.

Dunne, L.A., P.R. Manoogian and D.F. Pierini 1990. Structural style and domains of the northern Oman Mountains (Oman and United Arab Emirates). In A.H.F. Robertson, M.P. Searle and A.C. Ries (Eds.), The Geology and Tectonics of the Oman Region. Geological Society of London, Special Publication no. 49, p. 375-386.

Flemings, P.B. and T.E. Jordan 1989. A synthetic stratigraphic model of foreland basin development. Journal of Geophysical Research, v. 94, p. 3851-3866.

Glennie, K.W., M.G.A. Boeuf, M.W. Hughes Clark, M. Moody-Stuart, M.F. Pilaar and B.M. Reinhardt 1973. Late Cretaceous nappes in the Oman Mountains and their geological evolution. American Association of Petroleum Geologists Bulletin, v. 57, p. 5-27.

Hansen, S.E., A.J. Rodgers, S.Y. Schwartz and A.M.S. Al-Amri 2007. Imaging rupted lithosphere beneath the Red Sea and Arabian Peninsula. Earth and Planetary Sciences Letters, v. 259, p. 256-265.

Holt, W.E. and T.A. Stern 1991. Sediment loading on the western platform of the New Zealand continent: Implications for the strength of a continental margin. Earth and Planetary Sciences Letters, v. 107, p. 523-538.

Issler, D.R. 1992. A new approach to shale compaction and stratigraphic restoration, Beaufort-Mackenzie Basin and Mackenzie Corridor, northern Canada. American Association of Petroleum Geologists Bulletin, v. 76, p. 1170-1189.

Jordan, T. 2007. Gravity anomalies and flexure of the West Oman Foreland Basin: Implications for the thermal and mechanical evolution of continental lithosphere. DPhil, Oxford University, Oxford, UK.

Jordan, T.E. 1981. Thrust loads and foreland basin evolution, Cretaceous, western United States. American Association of Petroleum Geologists Bulletin, v. 65, p. 2506-2520.

Karner, G.D. and A.B. Watts 1983. Gravity anomalies and flexure of the lithosphere at mountain ranges. Journal of Geophysical Research, v. 88, p. 10,449-410,477.
Krishna, M.R., S. Chand and C. Subrahmanyam 2000. Gravity anomalies, sediment loading and lithospheric flexure associated with the Krishna-Godavari basin, eastern continental margin of India. Earth and Planetary Sciences Letters, v. 175, p. 223-232.
Lin, A.T. and A.B. Watts 2002. Origin of the West Taiwan basin by orogenic loading and flexure of a rifted continental margin. Journal of Geophysical Research, v. 107, 10.1029/2001JB000669.
Lippard, S.J., A.W. Shelton and I.G. Gass 1986. The Ophiolite of Northern Oman. Geological Society of London Memoir, v. 11, p. 1-178.
Liu, S.-F. and D. Nummedal 2004. Late Cretaceous subsidence in Wyoming: Quantifying the dynamic component. Geology, v. 32, p. 397-400.
McKenzie, D.P. 1978. Some remarks on the development of sedimentary basins. Earth and Planetary Sciences Letters, v. 40, p. 25-32.
Miller, K.G., M.A. Kominz, J.V. Browning, J.D. Wright, G.S. Mountain, M.E. Katz, P.J. Sugarman, B.S. Cramer, N. Christie-Blick and S.F. Parker 2005. The Phanerozoic Record of Global Sea-Level Change. Science, v. 310, p. 1293-1298.
Mitchum, R.M., P.R. Vail and J.B. Sangree 1977. Stratigraphic interpretation of seismic reflection patterns in depositional sequences. In C.E. Payton (Ed.), Seismic Stratigraphy – Applications to Hydrocarbon Exploration. American Association of Petroleum Geologists Memoir, v. 26, p. 117-133.
Noweir, M.A. and A. Alsharhan 2000. Structural style and stratigraphy of the Huwayyah anticline: An example of an Al-Ain Tertiary fold, northern Oman Mountains. GeoArabia, v. 5, no. 3, p. 387-402.
Osman, A. 2003. Late Campanian-Maastrichtian foraminifera from the Simsima Formation on the western side of the Northern Oman Mountains. Cretaceous Research, v. 24, p. 391-405.
Parsons, B.E. and J.G. Sclater 1977. An analysis of the variation of ocean floor bathymetry and heat flow with age. Journal of Geophysical Research, v. 82, p. 803-827.
Patton, T.L. and S.J. O'Connor 1988. Cretaceous flexural history of northern Oman mountain foredeep, United Arab Emirates. American Association of Petroleum Geologists Bulletin, v. 72, p. 797-809.
Perez-Gussinye, M., T.J. Reston and J. Phipps-Morgan 2001. Serpentinization and magmatism during extension at non-volcanic margins: The effect of initial lithospheric structure. In R.C.L. Wilson, et al. (Eds.), Non-Volcanic Rifting of Continental Margins. Geological Society of London, p. 551-576.
Pollastro, R. 2003. Total petroleum systems of the Paleozoic and Jurassic, Greater Ghawar Uplift and adjoining province of Central Saudi Arabia and Northern Arabian-Persian Gulf. United States Geological Survey Bulletin 2202-H.
Price, R.A. 1971. Gravitational sliding and the foreland thrust and fold belt of the North American Cordillera: Discussion. Geological Society of American Bulletin, v. 82, p. 1133-1138.
Rabu, D., P. Nehlig, J. Roger, F. Béchennec, M. Beurrier, J. LeMetour, C.H. Bourdillon-de-Grissac, M. Tegyey. J. Chauvel, C. Cavelier, H. Al-Azri, T. Juteau, D. Janjou, B. Lemiere, M. Villey and R. Wyns 1993. Stratigraphy and structure of the Oman Mountains. Bureau de Recherches Geologiques et Minieres, no. 221, Orleans, France.
Raiga-Clemenceau, J., J.P. Martin and S. Nicoletis 1988. The concept of acoustic formation factor for more accurate porosity determination from sonic transit data. Log Analyst, v. 29, p. 54-60.
Ravaut, P. and W. Warsi 1997. Bouguer anomaly map of Oman. Ministry of Petroleum and Minerals, Sultanate of Oman.
Robertson, A.H.F. 1987a. The transition from a passive margin to an Upper Cretaceous foreland basin related to ophiolite emplacement in the Oman Mountains. Geological Society of America Bulletin, v. 99, p. 633-653.
Robertson, A.H.F. 1987b. Upper Cretaceous Muti Formation: Transition of a Mesozoic carbonate platform to a foreland basin in the Oman Mountains. Sedimentology, v. 34, p. 1123-1142.
Robertson, A.H.F. and M.P. Searle 1990. The northern Oman Tethyan continental margin. In A.F.H. Robertson, M.P. Searle and A.C. Ries (Eds.), The Geology and Tectonics of the Oman Region. Geological Society of London, Special Publication no. 49, p. 3-25.
Robertson, A.H.F., C.D. Blome, D.W.J. Cooper, A.E.S. Kemp and M.P. Searle 1990. Evolution of the Arabian continental margin in the Dibba Zone, Northern Oman Mountains. In A.F.H. Robertson, M.P. Searle and A.C. Ries (Eds.), The Geology and Tectonics of the Oman Region. Geological Society of London, Special Publication no. 49, p. 251-284.
Rodger, M., A.B. Watts, C.J. Greenroyd, C. Peirce and R.W. Hobbs 2006. Evidence for unusually thin oceanic crust and strong mantle beneath the Amazon Fan. Geology, v. 34, p. 1081-1084.
Roure, F., J. Bruneau, L. Chérel, N. Elouz, J.-L. Faure, F. Girard, A. Jardin, C. Naville, S. Rodriguez and M. Tarapoanca 2006. Deep seismic survey in the Northern Emirates, Part II. Main Interpretation and Modelling Report. United Arab Emirates Ministry of Energy, Abu Dhabi, UAE.
Royden, L. and G.D. Karner 1984. Flexure of the lithosphere beneath Apennine and Carpathian foredeep basins: Evidence for an insufficient topographic load. American Association of Petroleum Geologists Bulletin, v. 68, p. 704-712.
Ruban, D.A., M.I. Al-Husseini and Y. Iwasaki 2007. Review of Middle East Paleozoic plate tectonics. GeoArabia, v. 12, no. 4, p. 35-56.
Savage, M. 2007. Gravity anomalies over the United Arab Emirates foreland and their tectonic implications. M.S. Oxford University, Oxford, UK.
Searle, M.P. 1988a. Thrust tectonics of the Dibba zone and the structural evolution of the Arabian continental margin along the Musandam Mountains (Oman and United Arab Emirates). Journal of the Geological Society of London, v. 145, p. 43-53.
Searle, M.P. 1988b. Structure of the Musandam culmination (Sultanate of Oman and United Arab Emirates) and the Straits of Hormuz syntaxis. Journal of the Geological Society of London, v. 145, p. 831-845.
Searle, M.P. 2007. Structural geometry, style and timing of deformation in the Hawasina Window, Al Jabal al Akhdar and Saih Hatat culminations, Oman Mountains. GeoArabia, v. 12, no. 2, p. 99-130.
Searle, M.P. and M.Y. Ali 2009. Structural and tectonic evolution of Jabal Sumeini- Al Ain – Buraimi region, northern Oman and eastern United Arab Emirates. GeoArabia, v. 14, no. 1, p. 113-140.
Searle, M.P., D.J.W. Cooper and K.F. Watts 1990. Structure of the Jebel Sumeini-Jebel Ghawil area, Northern Oman. In A.H.F. Robertson, M.P. Searle and A.C. Ries (Eds.), The Geology and Tectonics of the Oman Region. Geological Society of London, Special Publication no. 49, p. 361-374.
Searle, M.P. and J. Cox. 1999. Subduction zone metamorphism during formation and emplacement of the Semail ophiolite in the Oman Mountains. Geology Magazine, v. 139, p. 241-255.

Searle, M.P., N.P. James, T.J. Calon and J.D. Smewing 1983. Sedimentological and structural evolution of the Arabian continental margin in the Musandam Mountains and Dibba zone, United Arab Emirates. Geological Society of America Bulletin, v. 94, p. 1381-1400.
Sheriff, R.E. and L.P. Geldart 1995. Exploration seismology. Cambridge University Press, UK, p. 349-420.
Sinclair, H.D., B.J. Coakley, P.A. Allen and A.B. Watts 1991. Simulation of foreland basin stratigraphy using a diffusion model of mountain belt uplift and erosion: An example from the central Alps, Switzerland. Tectonics, v. 10, p. 599-620.
Skelton, P.W., S.C. Nolan and R.W. Scott 1990. The Maastrichtian transgression onto the northwestern flank of the Proto-Oman Mountains: Sequences of rudist-bearing beach to open shelf facies. In A.F.H. Robertson, M.P. Searle, A.C. Ries (Eds.), The Geology and Tectonics of the Oman Region. Geological Society of London, Special Publication no. 49, p. 521-547.
Steckler, M.S. and A.B. Watts 1978. Subsidence of the Atlantic-type continental margin off New York. Earth and Planetary Sciences Letters, v. 41, p. 1-13.
Styles, M.T., Ellison, R.A., S.L.B. Arkley, Q. Crowley, A. Farrant, K.M. Goodenough, J.A. Mckervey, T.C. Pharaoh, E.R. Philips, D. Schofield and R.J. Thomas 2006. The geology and geophysics of the United Arab Emirates. Volume 2: Geology. British Geological Survey.
Tilton, G.R., C.A. Hopson and J.E. Wright 1981. Uranium-lead isotopic ages of the Semail ophiolite, Oman with application to Tethyan ocean ridge tectonics. Journal of Geophysical Research, v. 86, p. 2763-75.
Ungerer, P., J. Burrus, B. Doligez, P.Y. Chenet and F. Bessis 1990. Basin evaluation by integrated two-dimensional modelling of heat transfer, fluid flow, hydrocarbon generation, and migration. American Association of Petroleum Geologists Bulletin, v. 74, p. 309-335.
Wapples, D.W. 1980. Time and temperature in petroleum formation: Application of Lapatin's method to petroleum exploration. American Association of Petroleum Geologists Bulletin, v. 64, p. 916-926.
Wapples, D.W. 2002. Maturity modelling: Thermal indicators, hydrocarbon generation, and oil cracking. In L.B. Magoon and W.G. Dow (Eds.), The Petroleum System - From Source to Trap. American Association of Petroleum Geologists, Memoir 60, p. 285-322.
Warburton, J., T.J. Burnhill, R.H. Graham and K.P. Isaac 1990. The evolution of the Oman Mountains foreland basin. In A.H.F. Robertson, M.P. Searle and A.C. Ries (Eds.), The Geology and Tectonics of the Oman Region. Geological Society of London, Special Publication no. 49, p. 419-427.
Warren, C.J., R.R. Parrish, M.P. Searle and D.J. Waters 2003. Dating the subduction of the Arabian continental margin beneath the Semail ophiolite, Oman. Geology, v. 31, p. 889-982.
Watts, A.B. and W.B.F. Ryan 1976. Flexure of the lithosphere and continental margin basins. Tectonophysics, v. 36, p. 25-44.
Watts, A.B. and M.S. Stecker 1979. Subsidence and eustasy at the continental margin of eastern North America. In M. Talwani, W. Hay and W.B.F. Ryan (Eds.), Deep Drilling Results in the Atlantic Ocean: Continental Margins and Paleoenvironment. Maurice Ewing Series 3: Washington, DC, American Geophysical Union, p. 218-234.
White, N. and D.P. McKenzie 1988. Formation of the "Steer's Head" geometry of sedimentary basins by differential stretching of the crust and mantle. Geology, v. 16, p. 250-253.

ABOUT THE AUTHORS

Mohammed Y. Ali *has a degree in Exploration Geology, an MSc in Geophysics, Postgraduate Certificate in Education, and a PhD in Marine Geophysics from Oxford University, UK. His current research projects are focused on exploration geophysics in the areas of seismic processing, passive seismic, seismic stratigraphy and reservoir characterisation and modelling. Other research interests include basin analysis, crustal studies, and the structure of passive margins. Mohammed joined The Petroleum Institute, Abu Dhabi, in 2003 as an Assistant Professor of Geophysics, previous to which he had been a Researcher at Oxford University. He is a member of the SEG, EAGE, AAPG and AGU.*

mali@pi.ac.ae

Anthony B. Watts *has a BSc in Geology and Physics from University College, London, a PhD in Marine Geophysics from Durham University, and a DSc from Oxford University, UK. His current research is focused on the gravity field and its relationship to isostasy, lithospheric flexure, and the thermal and mechanical evolution of sedimentary basins. Other research interests include marine geology and geophysics and the deep structure of continental margins, seamounts and oceanic islands, and mid-ocean ridges. Anthony joined Oxford University in 1991 as a Professor of Marine Geology and Geophysics, previous to which he had been the Arthur D. Storke Memorial Professor of Geology at Columbia University, New York, USA. He is a fellow of the AGU, GSA and EGU.*

tony@earth.ox.ac.uk

Manuscript received March 30, 2008
Revised June 27, 2008
Accepted July 10, 2008
Press version proofread by authors January 10, 2009